

Supplementary Information

Characterization of a thaumarchaeal symbiont that drives incomplete nitrification in the tropical sponge *Ianthella basta*

5 Florian U. Moeller, Nicole S. Webster, Craig W. Herbold, Faris Behnam, Daryl Domman, Mads
Albertsen, Maria Mooshammer, Stephanie Markert, Dmitrij Turaev, Dörte Becher, Thomas Rattei,
Thomas Schweder, Andreas Richter, Margarete Watzka, Per Halkjaer Nielsen, and Michael Wagner

Table of contents:

10

1. Supplementary Results and Discussion
2. Supplementary Experimental Procedures
3. Figures S1 – S7
4. Table S1-S5
- 15 5. References

Supplementary Results and Discussion

20 **High GC content of *Ca. Nitrosospongia bastadiensis*.** Both thaumarchaeal symbiont MAGs from *I. basta* possess the highest GC content (64.8%) of any genome-sequenced thaumarchaeote (Fig. 2C). While the GC content in the genome of *Ca. Cenarchaeum symbiosum* is similarly high (57.4%), the thaumarchaeal MAGs from the sponges *Cymbastela concentrica* (Moitinho-Silva *et al.*, 2017a) and a glass sponge (Tian *et al.*, 2016) had a much lower GC content (Fig. 2C). The high
25 GC content found in the *I. basta* thaumarchaeal symbiont is consistent with the high GC content

evident in Mediterranean sponge metagenomes (GC content 58-63%), particularly when compared to seawater metagenomes (GC content 41%) collected at the same location (Horn *et al.*, 2016).

Similarly, the GC content of six sponge microbiome metagenomes (Fan *et al.*, 2012) that we queried had an average GC content of $57.8\% \pm 6.7$ (SD), with three great barrier reef sponge species having an average microbiome metagenomic GC content of $63.3\% \pm 2.2$ (SD). In contrast, the average GC composition of selected marine and coral microbiomes are ~48% and ~45%, respectively (Reichenberger *et al.*, 2015). While several environmental factors are thought to affect the genomic GC content of bacteria and archaea (Foerstner *et al.*, 2005; Wang *et al.*, 2006), increased rates of homologous recombination via GC-biased gene conversion has recently been proposed as a crucial factor universally influencing the nucleotide content of microbial genes and genomes (Lassalle *et al.*, 2015). The possibility that sponge microbiomes are hot spots for input of novel genetic material via lateral gene transfer events (Fan *et al.*, 2012; Horn *et al.*, 2016), and also display increased homologous recombination rates should be assessed in future work.

Environmental distribution of *Ca. Nitrosospongia bastadiensis*. The *Ca. N. bastadiensis* 16S rRNA gene was queried against the Sponge Microbiome Project (SMP) database containing amplicon data sets from 268 sponge species including *I. basta* (Moitinho-Silva *et al.*, 2017b). The top hits were inserted into our reference 16S rRNA gene tree (Fig. 2A) using the Evolutionary Placement Algorithm (EPA; Berger *et al.*, 2011). 76 OTUs placed adjacent to the sponge-specific

sequence cluster 174, including one with 100% identity to *Ca. N. bastadiensis*. These 76 OTUs comprised, on average, $17.2\% \pm 7.1$ (SD) of all reads obtained from *I. basta* individuals in the SMP dataset, consistent with abundances determined by FISH and qPCR (see main text). Interestingly, the *Ca. N. bastadiensis*-adjacent OTUs were also found to comprise 0.25 – 7.5% of the total reads obtained from *Ancorina alata*, *Stellata maori*, *Stellata aremaria* sampled in New Zealand and *Xestospongia exigua* sampled on the Great Barrier Reef. In *X. exigua*, one low abundance OTU (0.17% of all reads) had 100% nucleotide identity with the V4 region of the *Ca. N. bastadiensis* 16S

rRNA gene. Among all environmental samples covered by the EMP, sequences highly similar or identical to *Ca. N. bastadiensis*, with abundances above 0.1%, were exclusively found in sponges. Consistent with a habitat restricted to a few sponge species, no hits above 97.6% similarity to the 55 16S rRNA gene of *Ca. N. bastadiensis* were detected by the Integrated Microbial NGS platform that queries most publicly available 16S rRNA gene amplicon data sets (but not the SMP dataset) (Lagkouvardos *et al.*, 2016).

Eukaryotic-like proteins (ELPs) in *Ca. Nitrosospongia bastadiensis*. Four types of ELPs are 60 found in *Ca. N. bastadiensis*: Proteins with tetratricopeptide repeats (TPR), the Toll-interleukin-1 receptor (TIR) -like domain PF08937 (DUF1863; Cort *et al.*, 2000), immunoglobulin-like (Ig-like) domains (DUF5011; Shigeno-Nakazawa *et al.*, 2016), and hyaline repeats (HYR; Callebaut *et al.*, 2000). The TPR were enriched in *Ca. N. bastadiensis* when compared to other genome sequenced thaumarchaeotes, while the TIR and Ig-like domains were exclusive to *Ca. N. bastadiensis* (Fig. 3, 65 Supporting Information Fig. S5). Of the TPR containing proteins in *Ca. N. bastadiensis*, 41 represent TPR gene families not previously detected in other thaumarchaeotes. TPR-containing proteins, which mediate protein-protein interactions in eukaryotes (Blatch and Lässle, 1999), are thought to be important for the survival of sponge symbionts in their phagocytic hosts. Two TPR-containing proteins from sponge microbiomes cloned into *E. coli* affected amoeba phagocytosis 70 (Reynolds and Thomas, 2016), however, both proteins contained the TPR-Sel1 motif which was absent in the TPR-containing proteins from *Ca. N. bastadiensis*. TIR-like proteins have also been found in other marine sponges (Wiens *et al.*, 2006; Gauthier *et al.*, 2010), with these proteins known to be key mediators of the metazoan innate immune response as well as playing a role in regulating metabolic and bioenergetic pathways through modulating NAD⁺ levels (Essuman *et al.*, 75 2018). TIR-like proteins were expressed when sponges were subjected to bacteria-analogue lipoproteins (Wiens *et al.*, 2006) and lipopolysaccharides (Wiens *et al.*, 2005), which in turn caused the expression of a caspase likely involved in apoptosis and a macrophage-expressed protein,

respectively. In this context, it is interesting to note that a protein encoding the DUF1863 domain from a zoonotic *Staphylococcus aureus* can decrease the survivability of mice infected by this strain
80 (Patterson *et al.*, 2014). Furthermore, the DUF1863 domain was recently shown to be a critical component of a bacterial defense system against myophages and may be involved in recognizing specific phage patterns (Doron *et al.*, 2018).

An evolutionary homology between choanoflagellates and sponge choanocytes has long been speculated (Maldonado, 2005; Mah *et al.*, 2014; Laundon *et al.*, 2018). Both have diverse and
85 abundant receptor tyrosine kinases (RTKs) (Srivastava *et al.*, 2010; Miller, 2012), which are crucial components of metazoan signal transduction systems. Interestingly, choanoflagellate proteins with HYR-like domains were recently predicted to act as receptor tyrosine kinases (RTKs) (Manning *et al.*, 2008). As HYR domains are structurally related to Ig and FN3 domains (Callebaut *et al.*, 2000) and choanoflagellates lack the Ig domains found in many metazoan RTKs, the HYR domains may
90 be fulfilling the role of the Ig domains in metazoan RTKs. Furthermore, the Ig-like DUF5011 domain has been found on the extracellular portion of two choanoflagellate homologues of the tyrosine kinase substrate BCAR1 (Shigeno-Nakazawa *et al.*, 2016). Consequently, the numerous DUF5011 and HYR domain containing proteins of *Ca. N. bastadiensis* may be interacting with the host signaling network as *I. basta* likely harbors similar extracellular domains as part of its signal
95 transduction and gene regulatory processes. This host-symbiont interaction is further supported by observations that (i) many *Ca. N. bastadiensis* proteins encoding these domains are predicted to be exported and (ii) five extracellular proteins of the *Ca. N. bastadiensis* exclusive gene family containing the DUF5011 domain were detected in the metaproteome (Supporting Information Table S3).

100

Supplementary Experimental Procedures

105 **Phylogenetic analyses.** S-layer proteins were identified in all sequenced thaumarchaeota based on orthologous groups identified with Orthofinder containing members previously identified as SLPs (Li *et al.*, 2018), or also classified as arCOG08647 in EggNOG version 4.5 (Huerta-Cepas *et al.*, 2016). A phylogenetic reconstruction was performed with a thaumarchaeal-specific dataset with a minimal sequence length of 300 amino acids. Sequences were aligned using mafft (Katoh and Standley, 2013) and automatically trimmed using trimAl version 1.4 (Capella-Gutiérrez *et al.*, 2009) and the -gappyout function. After model selection using ModelFinder (Kalyaanmoorthy *et al.*, 2017) and a maximum-likelihood amino acid phylogenetic tree was generated using the model LG+F+G4 in IQ-Tree, version 1.6.2 (Nguyen *et al.*, 2015) with 1,000 ultrafast bootstraps (UFBoot).

110 Genes encoding S08A family endopeptidases were identified in all sequenced thaumarchaeota if they contained the PF00082 (Peptidase_S8) domain when searched against the Pfam-A database. The complete sequence set was identified using thaumarchaeal amino acid sequences as individual queries for blastp searches against the Genbank nr database and only top hits containing the PF00082 domain were included. In total 277 representative sequences of the S08A family endopeptidases were used for phylogenetic analyses and sequences were trimmed according to the presence of the PF00082 domain before alignment using mafft (Katoh and Standley, 2013). ModelFinder (Kalyaanmoorthy *et al.*, 2017) was used for model selection and maximum-likelihood phylogenetic analyses implemented with IQ-Tree, version 1.6.2 (Nguyen *et al.*, 2015), using the LG+I+G4 model and 1,000 ultrafast bootstraps (UFBoot). Phylogenetic analyses for serpins (PF00079) were conducted in a similar fashion and 75 representative sequences were analyzed (after filtering out 46 distant homologues) using the WAG+I+G4 model and 1,000 ultrafast bootstraps.

Phylogenetic analyses were conducted on amino acid sequences of the *LivK* periplasmic branched chain amino acid transporter subunit as well as a concatenated alignment of the *LivFGHMK* operon, using the best model identified for each dataset by ModelFinder
130 (Kalyaanmoorthy *et al.*, 2017) and implemented in IQ-Tree, version 1.6.2 (Nguyen *et al.*, 2015) with 1,000 ultrafast bootstraps (UFBoot). The complete sequence set was identified using individual *Ca. N. bastadiensis* *LivFGHMK* operon subunits as individual queries for blastp searches against the Genbank nr database. Top hits were included along with additional sequences demonstrated to be functional for active substrate transport within the hydrophobic amino-acid uptake transporter
135 (HAAT) family (TCDB:3.A.14; Saier *et al.*, 2009). Sequences were aligned using mafft (Katoh and Standley, 2013) and automatically trimmed using trimAl version 1.4 (Capella-Gutiérrez *et al.*, 2009) and the -gappyout function. Models used for maximum-likelihood phylogenetic analyses were LG+F+G4 and LG+F+I+G4 for the *LivK* subunit and the concatenated *livFGHMK* operon, respectively.

140

Database screening for 16S rRNA gene amplicons. A reference set of 16S rRNA gene sequences (N=65) from sequenced thaumarchaeotal genomes and amplicons associated with sponges, including *Ca. N. bastadensis* were aligned with SINA (Pruesse *et al.*, 2012) and used to construct a reference tree in RaXML (Stamatakis, 2014). Sequence tags identified by the Sponge Microbiome
145 Project (Moitinho-Silva *et al.*, 2017b) were mapped to the reference set using blastn (Camacho *et al.*, 2009), requiring at least 70% alignment and 90% identity. Successfully mapped reads were then aligned to the reference alignment using SINA and placed into the reference tree using RaXML-EPA (Berger *et al.*, 2011). In addition, 16S rRNA gene sequences related to *Ca. N. bastadensis* were identified in short read archive (SRA) datasets using IMNGS (www.imngs.org - Lagkouvardos *et al.*, 2016) with default parameters.

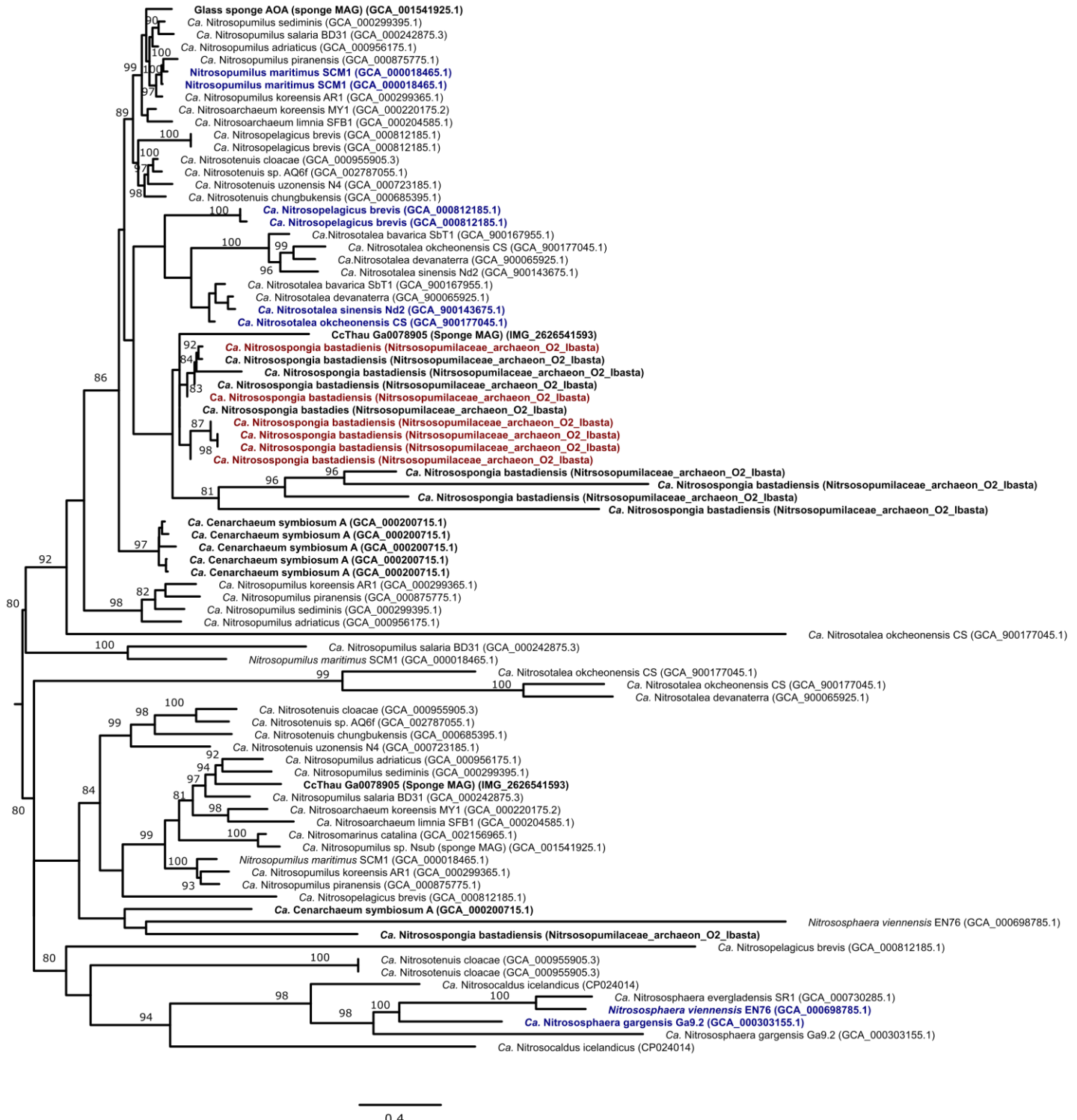


Figure S1. Maximum-likelihood amino acid phylogenetic tree (after automatic model selection with IQ-Tree, version 1.6.2) of putative S-layer proteins found in all analyzed thaumarchaeal genomes (28 in total). Sponge-derived sequences are depicted in bold black, while highly expressed proteins from *Ca. N. bastadiensis* are depicted in bold red (6 in total). Highlighted in bold blue are putative S-layer proteins found to be highly expressed in previous proteomics studies (Santoro *et al.*, 2015; Palatinszky *et al.*, 2015; Kerou *et al.*, 2016; Qin *et al.*, 2017; Herbold *et al.*, 2017). Values at nodes represent ultrafast bootstraps (UFBoot) with only values $\geq 80\%$ shown for each branch.

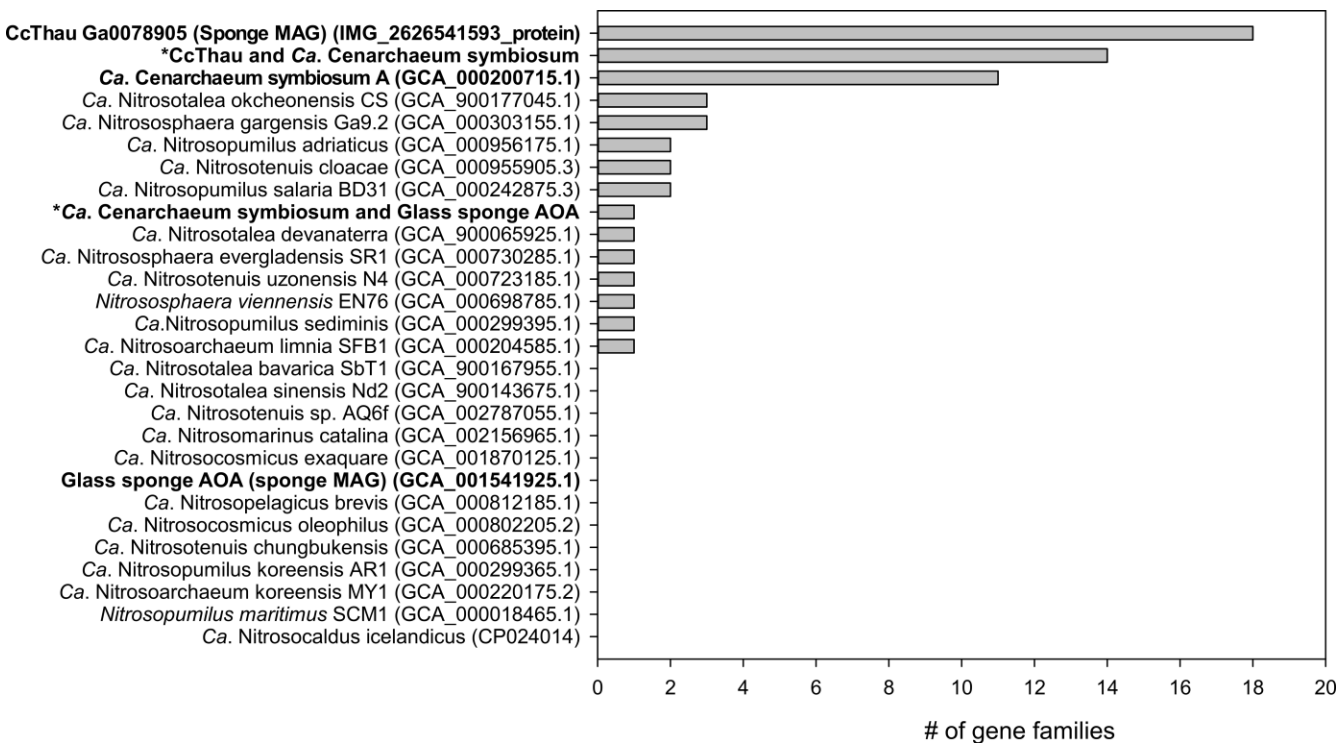
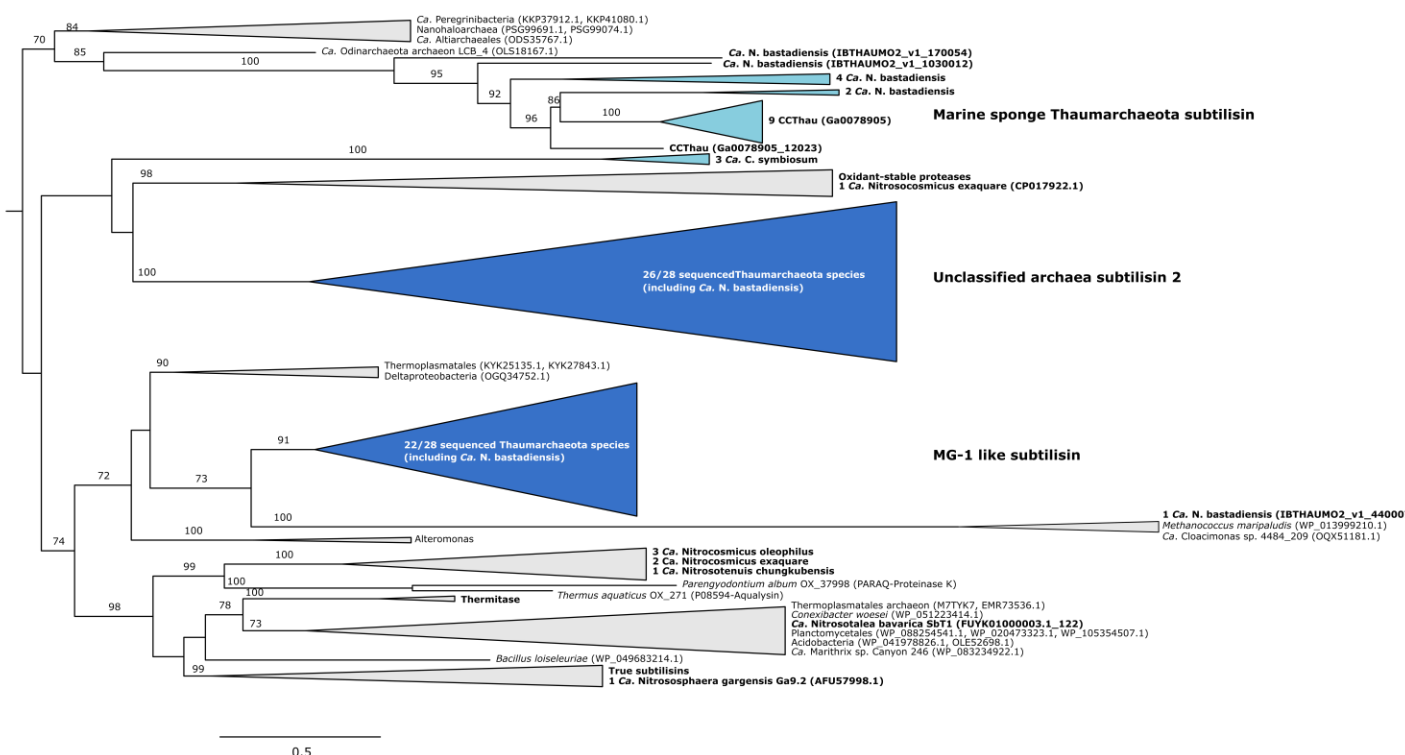


Figure S2. Number of gene families shared exclusively between *Ca. N. bastadiensis* and each genome-sequenced member of the *Thaumarchaeota* including the sponge thaumarchaeal symbionts, CCThau, *Ca. C. symbiosum*, and the glass sponge AOA (in bold). (*) indicates gene families shared by *Ca. N. bastadiensis* with *Ca. C. symbiosum* and CCThau exclusively, or with *Ca. C. symbiosum* and the glass sponge AOA exclusively.

A



B

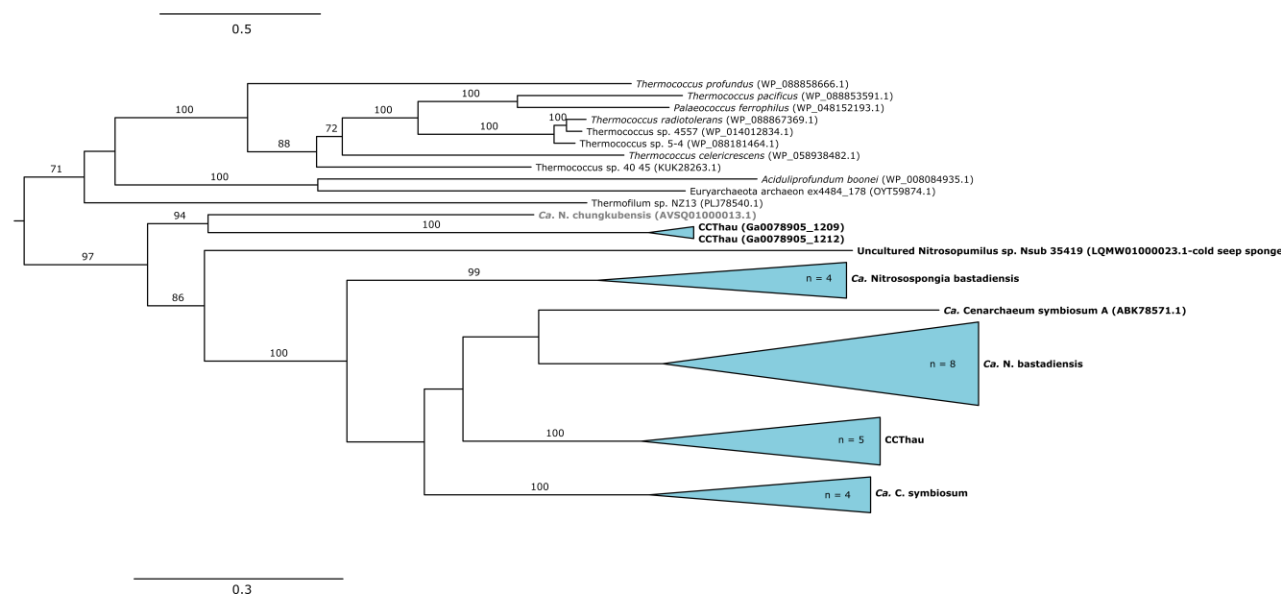
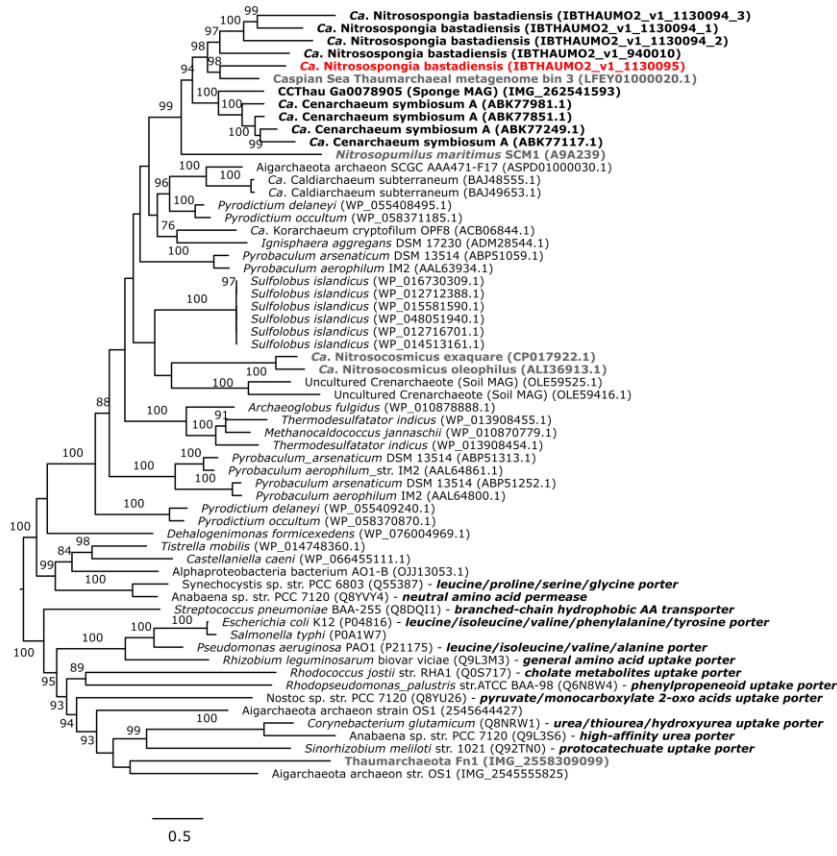


Figure S3. Maximum-likelihood amino acid phylogenetic trees (after automatic model selection with IQ-Tree, version 1.6.2) of (A) S08A family endopeptidases and (B) serine protease inhibitors (serpins). Color coding donates the degree of homology among all sequenced *Thaumarchaeota*: light blue – shared exclusively among thaumarchaeal sponge symbionts; dark blue – ubiquitously found in *Thaumarchaeota*. In (A), 6 out of 8 *Ca. N. bastadiensis* S08A family endopeptidases, within the “Marine sponge Thaumarchaeota subtilisin” clade, are predicted to be exported. On the other hand, the majority of the ubiquitous “Unclassified archaea subtilisin 2” (24/27) and all except one of the “MG-1 like subtilisin” (naming convention after Li *et al.*, 2015) are predicted to be membrane anchored S08A endopeptidases. In (B), 3 of the 15 serpins found in *Ca. N. bastadiensis* were excluded from phylogenetic analyses due to truncated length. Values at nodes represent ultrafast bootstraps (UFBoot) with only values $\geq 80\%$ shown for each branch.

A



B

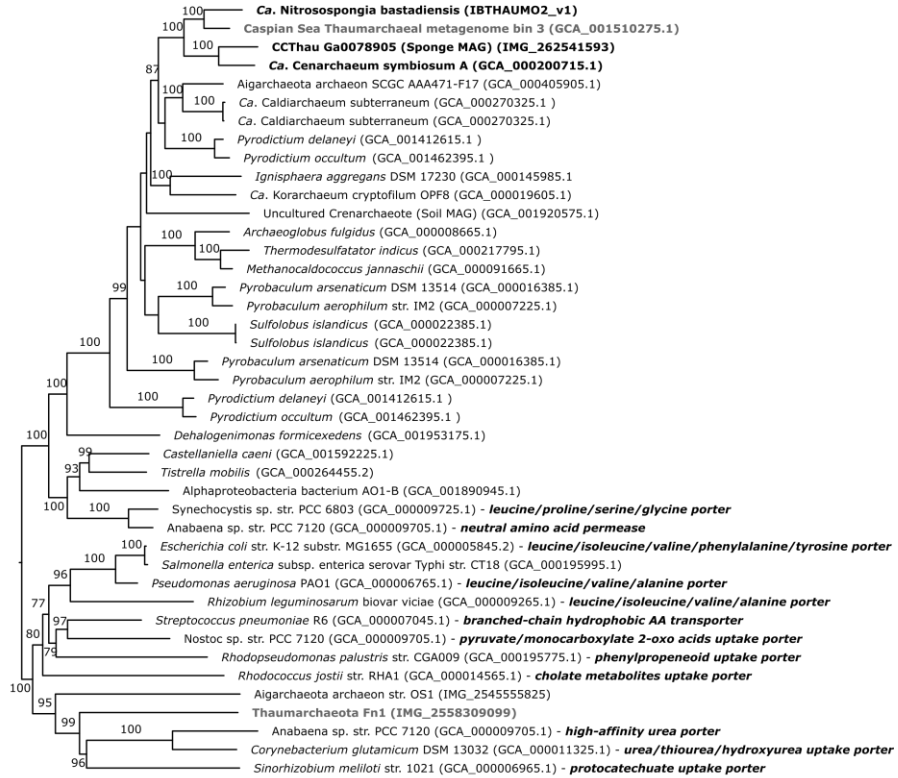


Figure S4. Maximum-likelihood amino acid phylogenetic trees (after automatic model selection with IQ-Tree, version 1.6.2) for the periplasmic subunit (A) *LivK* and for the concatenated (B) *LivFGHMK* operon. *LivK* was found to be highly expressed (expressed copy in red) in the *Ca. N. bastadiensis* proteome and can occur in multiple copies among *LivFGHMK* encoding microorganisms. *Ca. N. bastadiensis* has two *LivK* genes and a gene containing three fused *LivK* domains and the predicted proteins from these five *LivK* genes/domains were included in the phylogenetic analysis. *LivK* is also found in some other thaumarchaeotes (bold grey), but these lack the *LivFGHM* genes necessary for branched-chain amino acid transport. In a few cases in the concatenated *LivFGHMK* tree, multiple operons were present in a given genome. For both trees, sponge thaumarchaeal sequences are highlighted in bold black while other thaumarchaeal sequences are highlighted in bold grey. Sequences from organisms where the specific transport functions have been identified, have those specific functions annotated. These annotations are taken from information collated in the Transporter Classification database (Saier *et al.*, 2009). Values at nodes represent ultrafast bootstraps (UFBoot) with only values $\geq 80\%$ shown for each branch.

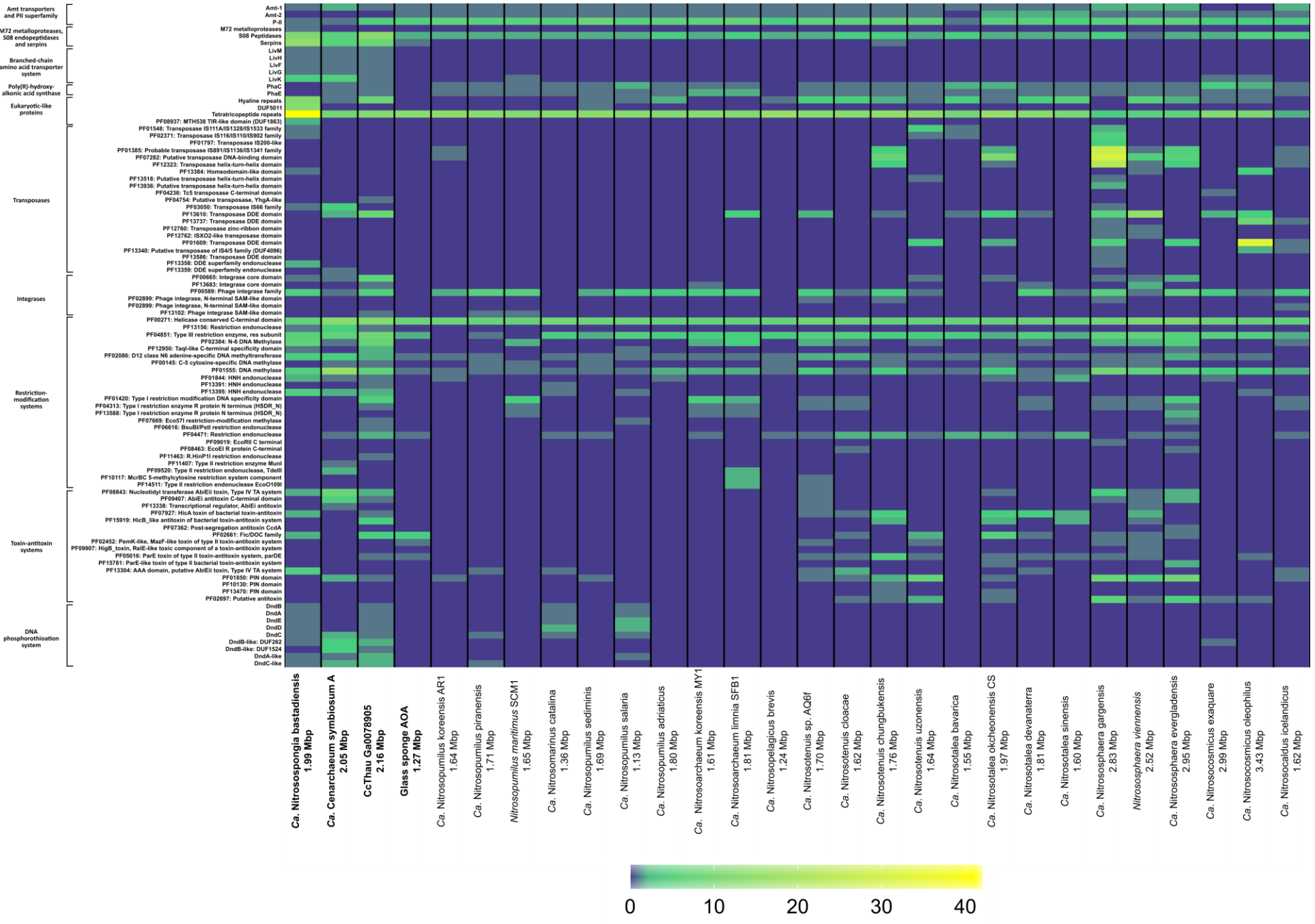


Figure S5. Heat map showing the distribution and gene copy number per genome of selected genes, gene classes and PFAM annotations among genome-sequenced AOA. The color scale ranges from 0 (dark blue) to 40 (yellow) and indicates copies per genome. Sponge-derived genomes start on the left and are depicted in bold, followed by members of *Ca. Nitrosopumilaceae*, *Ca. Nitrosotenuaceae*, *Ca. Nitrosotaleale*, the *Nitrososphaerales*, and *Ca. Nitrosocaldales*, respectively. Genome sizes for each member are listed below each name.

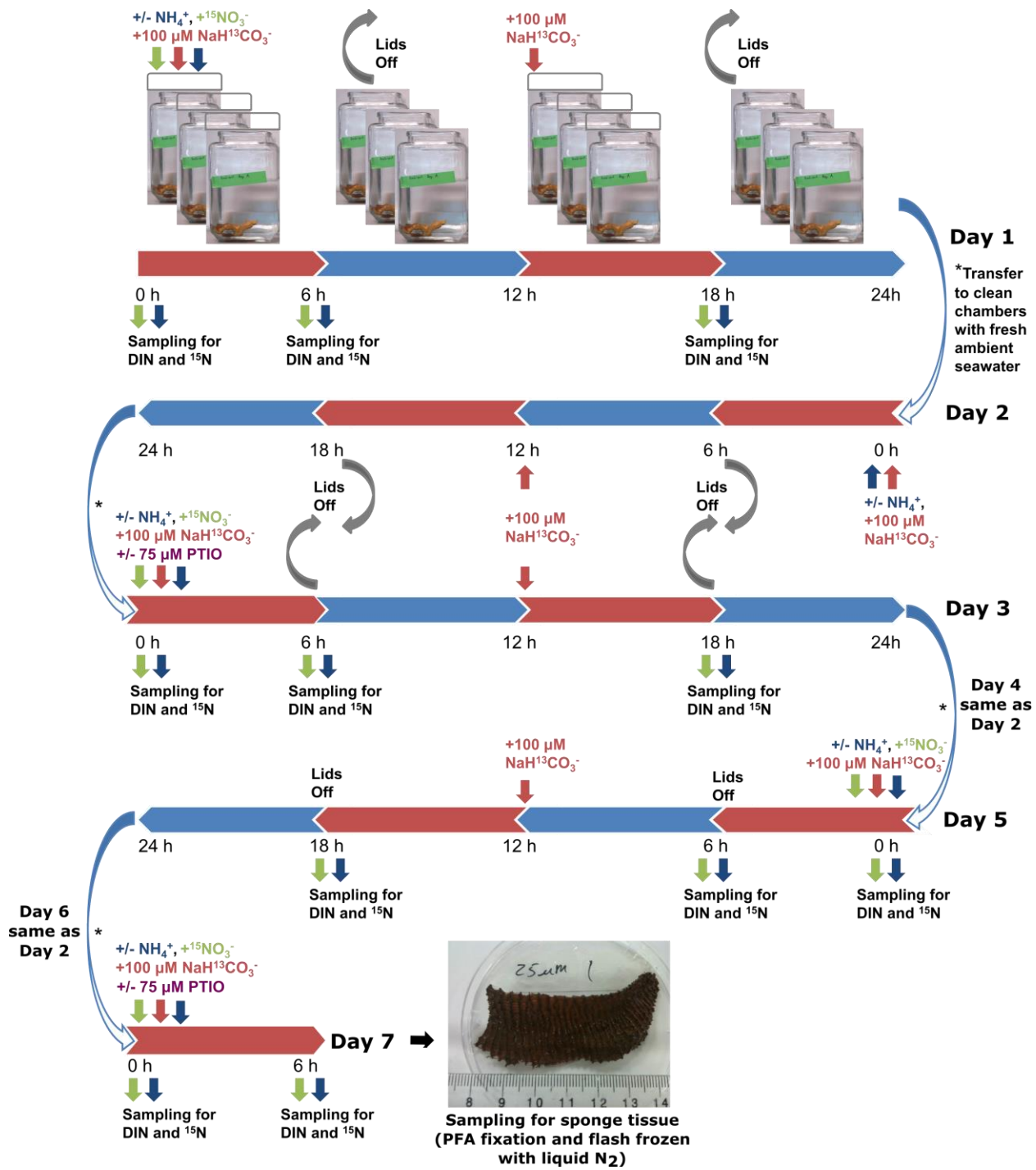


Figure S6. Experimental design for the *I. basta* holobiont nitrification incubations. The intermittently closed setup was employed to avoid oxygen depletion while minimizing loss of ^{13}C -labeled HCO_3^- . Green and blue arrows denote samples used for the calculation of net and gross nitrification rates, respectively. Days 4, 5 and 6 were recovery days for those incubations to which PTIO was added.

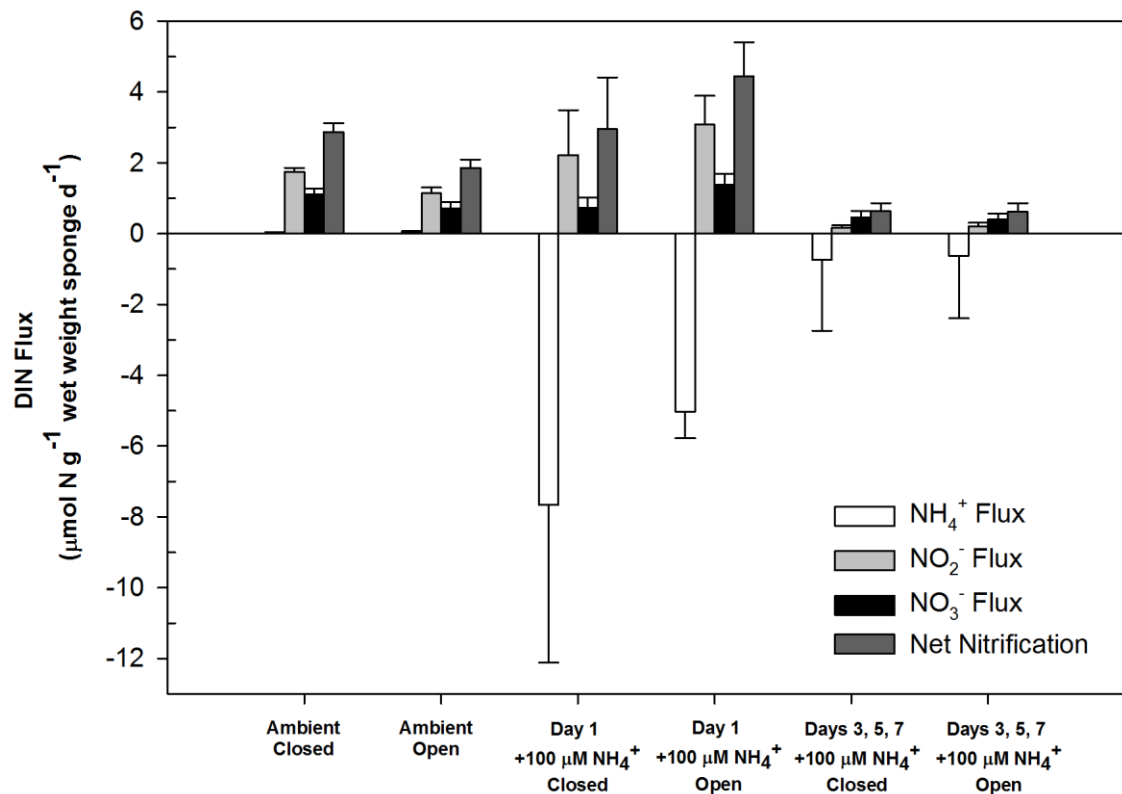


Figure S7. Comparison of average DIN (NH_4^+ , NO_3^- , NO_2^-) flux and net nitrification rates exhibited by the *I. basta* holobiont in multiple-day incubations between intermittently closed (Supplementary Figure 1) and completely open aquaria at ambient conditions and at 100 $\mu\text{M NH}_4^+$. Pair-wise comparisons of individual DIN species flux and net nitrification between open and intermittently closed aquaria, revealed significant differences in net NO_2^- flux and net nitrification between ambient treatments (both: $p < 0.01$, Mann-Whitney U-test).

Table S1. Overview of genome binning parameters, statistics and associated metadata for the *Ca. N. bastadiensis* genome bin.

Bin ID	IBThaumO2
Analysis project type	metagenome-assembled genome (MAG)
Taxa_id	16S rRNA and multi-marker phylogenetics
Assembly software	Spades
Annotation	MaGe
Genome Quality	High Quality Draft
Completeness (%)	99.03
Contamination (%)	0.97
Completeness/Contamination Software	CheckM
Number of contigs	113
16S rRNA gene recovered	yes
16S rRNA gene recovery software	Rnammer / MaGe
Number of standard tRNAs extracted	20
tRNA extraction software	tRNA-scan / MaGe
Binning software	metabat2
Binning parameters	kmer
Genome size (Mbp)	1.99
N50 (bp)	35099
Longest contig (bp)	135,585
Average contig length (bp)	17,669.70
GC content (%)	64.8
Protein coding sequences	2,342
rRNAs	3
tRNAs	42

Table S2. Presence of genes of interest (see Figure 3) in the two *Ca. N. bastadiensis* MAGs (obtained from two *I. basta* individuals by Illumina and 454 pyrosequencing, respectively) as determined by BLASTp.

	qseqid	sseqid	pident	length	qlen	slen	evalue	bitscore	query match coverage	subject match coverage
M72 metalloproteases	IBTHAUMO2_v1_880008	IBTHAUMv1_16080007	64.242	660	2028	2440	0	729	32.54	26.76
S08 Peptidases	IBTHAUMO2_v1_1030012	IBTHAUMv1_12290002	91.578	5141	5956	6201	0	9250	86.32	82.26
	IBTHAUMO2_v1_150018	IBTHAUMv1_17130004	99.286	560	908	611	0	1133	61.67	91.49
	IBTHAUMO2_v1_160002	IBTHAUMv1_1950001	100	659	1181	1349	0	1355	55.80	48.78
	IBTHAUMO2_v1_170054	IBTHAUMv1_3990003	99.646	1695	1695	1695	0	3440	100.00	99.94
	IBTHAUMO2_v1_220007	IBTHAUMv1_13830026	99.542	655	655	655	0	1257	100.00	99.85
	IBTHAUMO2_v1_250004	IBTHAUMv1_4210010	65.672	268	303	1619	1.16E-98	315	88.45	16.24
	IBTHAUMO2_v1_440007	IBTHAUMv1_14780018	99.856	696	699	696	0	1429	99.57	99.86
	IBTHAUMO2_v1_470031	IBTHAUMv1_15480003	99.794	1459	1459	1459	0	2938	100.00	99.93
	IBTHAUMO2_v1_470037	IBTHAUMv1_15480010	99.446	1264	1264	1266	0	2486	100.00	99.76
	IBTHAUMO2_v1_600001	IBTHAUMv1_1950001	89.893	1029	1563	1349	0	1843	65.83	76.20
Serpins	IBTHAUMO2_v1_810001	IBTHAUMv1_16080007	92.872	2413	2385	2440	0	4403	101.17	98.11
	IBTHAUMO2_v1_1040003	IBTHAUMv1_16780011	78.208	413	472	412	0	620	87.50	99.76
	IBTHAUMO2_v1_150002	IBTHAUMv1_9590002	100	412	412	412	0	835	100.00	99.76
	IBTHAUMO2_v1_150006	IBTHAUMv1_2680003	99.589	487	487	487	0	979	100.00	99.79
	IBTHAUMO2_v1_150019	IBTHAUMv1_17130003	100	468	501	499	0	943	93.41	93.59
	IBTHAUMO2_v1_160001	IBTHAUMv1_15480013	98.14	645	646	649	0	1268	99.85	99.23
	IBTHAUMO2_v1_250003	IBTHAUMv1_9590002	83.846	390	413	412	0	665	94.43	92.48
	IBTHAUMO2_v1_250005	IBTHAUMv1_3270002	50.427	117	107	377	4.53E-25	94.4	109.35	30.77
	IBTHAUMO2_v1_470041	IBTHAUMv1_17030009	92.308	273	389	649	0	521	70.18	41.91
	IBTHAUMO2_v1_470042	IBTHAUMv1_16080008	74.297	498	498	498	0	667	100.00	99.20
	IBTHAUMO2_v1_530010	IBTHAUMv1_3270002	97.706	218	240	377	3.43E-150	421	90.83	57.56
	IBTHAUMO2_v1_530011	IBTHAUMv1_3270002	98.052	154	154	377	7.63E-104	299	100.00	40.58
	IBTHAUMO2_v1_630004	IBTHAUMv1_4530014	100	419	419	419	0	853	100.00	99.76
	IBTHAUMO2_v1_740001	IBTHAUMv1_2680003	95.833	72	74	487	2.60E-36	124	97.30	14.58
	IBTHAUMO2_v1_810003	IBTHAUMv1_16080004	100	474	474	474	0	970	100.00	99.79
	IBTHAUMO2_v1_880009	IBTHAUMv1_16080008	100	498	498	498	0	1014	100.00	99.80
LivM	IBTHAUMO2_v1_1130089	IBTHAUMv1_13040008	99.717	353	353	353	0	677	100.00	99.72
LivH	IBTHAUMO2_v1_1130090	IBTHAUMv1_13040007	100	306	306	306	0	587	100.00	99.67
LivF	IBTHAUMO2_v1_1130093	IBTHAUMv1_13040004	100	238	238	238	1.80E-172	471	100.00	99.58
LivG	IBTHAUMO2_v1_1130092	IBTHAUMv1_13040005	99.209	253	269	253	0	496	94.05	99.60

LivK	IBTHAUMO2_v1_1130094	IBTHAUMv1_13040003	99.688	642	1149	642	0	1236	55.87	99.84
LivK	IBTHAUMO2_v1_1130095	IBTHAUMv1_16960002	93.738	527	527	511	0	993	100.00	99.80
LivK	IBTHAUMO2_v1_940010	IBTHAUMv1_330001	100	314	402	314	0	622	78.11	99.68
DndB	IBTHAUMO2_v1_810011	IBTHAUMv1_190016	44.688	320	362	319	2.21E-98	292	88.40	98.43
DndA	IBTHAUMO2_v1_880013	IBTHAUMv1_140010	70.712	379	391	388	0	566	96.93	97.42
DndE	IBTHAUMO2_v1_880014	IBTHAUMv1_140009	39.655	116	123	126	1.18E-32	108	94.31	91.27
DndD	IBTHAUMO2_v1_880015	IBTHAUMv1_190014	34.074	675	675	660	1.80E-107	337	100.00	99.55
DndC	IBTHAUMO2_v1_880016	IBTHAUMv1_140006	56.592	493	473	502	0	576	104.23	98.01
DndB-like: DUF262	IBTHAUMO2_v1_1050033	IBTHAUMv1_380002	27.711	166	425	344	2.67E-10	58.9	39.06	44.48
DndA-like	IBTHAUMO2_v1_690025	IBTHAUMv1_3820004	99.482	386	386	386	0	772	100.00	99.74
DndC-like	IBTHAUMO2_v1_690027	IBTHAUMv1_17710003	100	280	280	280	0	582	100.00	99.64
PF08937: MTH538 TIR-like	IBTHAUMO2_v1_460006	IBTHAUMv1_14780023	100	130	130	170	7.13E-94	265	100.00	75.88
	IBTHAUMO2_v1_620008	IBTHAUMv1_14750015	100	172	172	172	3.99E-126	349	100.00	99.42
Hyaline repeats	IBTHAUMO2_v1_150018	IBTHAUMv1_17130004	99.286	560	908	611	0	1133	61.67	91.49
	IBTHAUMO2_v1_1050019	IBTHAUMv1_14910004	99.774	442	442	442	0	880	100.00	99.77
	IBTHAUMO2_v1_1050020	IBTHAUMv1_14910005	75.036	701	705	702	0	988	99.43	99.15
	IBTHAUMO2_v1_1110002	IBTHAUMv1_460002	44.798	471	491	487	8.48E-124	368	95.93	96.51
	IBTHAUMO2_v1_1110003	IBTHAUMv1_15140009	49.099	444	443	452	2.55E-124	366	100.23	97.35
	IBTHAUMO2_v1_220002	IBTHAUMv1_150003	86.853	715	712	715	0	1217	100.42	99.86
	IBTHAUMO2_v1_450016	IBTHAUMv1_3920005	97.511	442	630	442	0	862	70.16	99.77
	IBTHAUMO2_v1_470043	IBTHAUMv1_16080007	92.531	241	237	2440	1.02E-125	389	101.69	9.80
	IBTHAUMO2_v1_720042	IBTHAUMv1_14780010	48.347	242	268	742	1.76E-63	209	90.30	31.81
	IBTHAUMO2_v1_810001	IBTHAUMv1_16080007	92.872	2413	2385	2440	0	4403	101.17	98.11
	IBTHAUMO2_v1_880008	IBTHAUMv1_16080007	64.242	660	2028	2440	0	729	32.54	26.76
PF16403: DUF5011	IBTHAUMO2_v1_1030012	IBTHAUMv1_12290002	91.578	5141	5956	6201	0	9250	86.32	82.26
	IBTHAUMO2_v1_170054	IBTHAUMv1_3990003	99.646	1695	1695	1695	0	3440	100.00	99.94
	IBTHAUMO2_v1_20012	IBTHAUMv1_11360007	95.513	936	1651	962	0	1722	56.69	97.19
	IBTHAUMO2_v1_240080	IBTHAUMv1_11360001	98.649	2073	2073	2073	0	4182	100.00	99.95
	IBTHAUMO2_v1_290009	IBTHAUMv1_13830036	99.644	1966	1966	1966	0	3962	100.00	99.95
	IBTHAUMO2_v1_320050	IBTHAUMv1_2050001	97.937	1115	1328	1117	0	2196	83.96	99.73
	IBTHAUMO2_v1_460001	IBTHAUMv1_14780028	91.978	1633	1773	4551	0	2982	92.10	35.62
	IBTHAUMO2_v1_470031	IBTHAUMv1_15480003	99.794	1459	1459	1459	0	2938	100.00	99.93
	IBTHAUMO2_v1_590001	IBTHAUMv1_20280001	98.699	615	648	1427	0	1256	94.91	43.03
	IBTHAUMO2_v1_590078	IBTHAUMv1_13120027	99.522	837	1040	848	0	1659	80.48	98.58

	IBTHAUMO2_v1_620022	IBTHAUMv1_12370012	98.862	1845	1845	2170	0	3714	100.00	84.98
	IBTHAUMO2_v1_700001	IBTHAUMv1_18570002	76.798	2836	3095	8426	0	4177	91.63	33.54
	IBTHAUMO2_v1_990001	IBTHAUMv1_4410003	99.731	1116	1116	11182	0	2271	100.00	9.97
Tetratricopeptide repeats	IBTHAUMO2_v1_20005	IBTHAUMv1_4210007	100	542	542	561	0	1096	100.00	96.43
	IBTHAUMO2_v1_260017	IBTHAUMv1_1700002	99.743	389	389	394	0	786	100.00	98.48
	IBTHAUMO2_v1_450009	IBTHAUMv1_15960007	98.947	665	665	665	0	1304	100.00	99.85
	IBTHAUMO2_v1_590071	IBTHAUMv1_13120019	98.704	463	463	463	0	926	100.00	99.78
	IBTHAUMO2_v1_690013	IBTHAUMv1_11050005	100	236	236	236	4.75E-174	475	100.00	99.58
	IBTHAUMO2_v1_250010	IBTHAUMv1_1040006	97.196	214	214	214	2.07E-147	406	100.00	99.53
	IBTHAUMO2_v1_590041	IBTHAUMv1_4080009	98.78	738	738	738	0	1435	100.00	99.86
	IBTHAUMO2_v1_730001	IBTHAUMv1_5300001	97.778	90	123	144	3.63E-61	181	73.17	61.81
	IBTHAUMO2_v1_1130054	IBTHAUMv1_13940010	100	262	262	262	0	514	100.00	99.62
	IBTHAUMO2_v1_10010	IBTHAUMv1_1840004	33.738	412	416	754	3.80E-61	208	99.04	54.24
	IBTHAUMO2_v1_1080005	IBTHAUMv1_16190004	99.153	118	118	118	1.76E-83	237	100.00	99.15
	IBTHAUMO2_v1_1120015	IBTHAUMv1_5290001	59.541	566	738	565	0	629	76.69	99.47
	IBTHAUMO2_v1_170044	IBTHAUMv1_3990013	99.425	174	174	174	1.18E-117	328	100.00	99.43
	IBTHAUMO2_v1_200001	IBTHAUMv1_15480023	99.693	326	417	326	0	643	78.18	99.69
	IBTHAUMO2_v1_20006	IBTHAUMv1_4210006	100	495	495	495	0	997	100.00	99.80
	IBTHAUMO2_v1_260040	IBTHAUMv1_1140003	99.635	274	274	274	0	539	100.00	99.64
	IBTHAUMO2_v1_330008	IBTHAUMv1_17060002	94.872	429	457	443	0	805	93.87	96.61
	IBTHAUMO2_v1_410008	IBTHAUMv1_13120019	45.02	251	274	463	1.19E-66	212	91.61	52.92
	IBTHAUMO2_v1_410009	IBTHAUMv1_1610001	94.574	387	399	394	0	697	96.99	97.97
	IBTHAUMO2_v1_440013	IBTHAUMv1_14780004	86.288	598	598	598	0	1035	100.00	99.83
	IBTHAUMO2_v1_450076	IBTHAUMv1_15360002	100	299	299	299	0	563	100.00	99.67
	IBTHAUMO2_v1_480001	IBTHAUMv1_3180004	100	339	339	339	0	669	100.00	99.71
	IBTHAUMO2_v1_480002	IBTHAUMv1_3180005	99.76	416	434	416	0	793	95.85	99.76
	IBTHAUMO2_v1_510001	IBTHAUMv1_2270002	100	279	279	534	0	553	100.00	52.06
	IBTHAUMO2_v1_690014	IBTHAUMv1_11050004	98.305	236	236	236	9.73E-172	469	100.00	99.58
	IBTHAUMO2_v1_650002	IBTHAUMv1_20210002	100	262	262	262	0	516	100.00	99.62
	IBTHAUMO2_v1_700005	IBTHAUMv1_21200002	96.032	252	256	256	4.84E-171	469	98.44	98.05
	IBTHAUMO2_v1_750012	IBTHAUMv1_2270002	100	241	243	534	4.86E-176	492	99.18	44.94
	IBTHAUMO2_v1_790015	IBTHAUMv1_15480026	99.77	435	435	435	0	852	100.00	99.77
	IBTHAUMO2_v1_880020	IBTHAUMv1_2270002	99.17	241	268	534	1.46E-174	489	89.93	44.94
	IBTHAUMO2_v1_940002	IBTHAUMv1_4830003	96.811	439	439	439	0	838	100.00	99.77

	IBTHAUMO2_v1_990018	IBTHAUMv1_16760014	100	140	140	140	2.46E-92	261	100.00	99.29
	IBTHAUMO2_v1_200002	IBTHAUMv1_15480022	93.885	278	283	286	4.26E-178	489	98.23	96.85
	IBTHAUMO2_v1_20010	IBTHAUMv1_4210003	98.396	187	187	187	1.12E-126	352	100.00	99.47
	IBTHAUMO2_v1_720008	IBTHAUMv1_4130013	100	127	127	127	1.21E-88	250	100.00	99.21
	IBTHAUMO2_v1_380029	IBTHAUMv1_11240003	100	309	309	309	0	606	100.00	99.68
	IBTHAUMO2_v1_590042	IBTHAUMv1_4080008	99.286	420	423	423	0	845	99.29	99.05
	IBTHAUMO2_v1_990017	IBTHAUMv1_16760013	100	68	68	68	7.21E-43	130	100.00	98.53
	IBTHAUMO2_v1_480009	IBTHAUMv1_90003	100	197	197	237	5.88E-143	395	100.00	82.70
	IBTHAUMO2_v1_700003	IBTHAUMv1_20360001	100	204	204	252	2.91E-149	412	100.00	80.56
Transposases	IBTHAUMO2_v1_1050022	IBTHAUMv1_8580062	99.457	368	368	368	0	733	100.00	99.73
	IBTHAUMO2_v1_560020	IBTHAUMv1_23780003	100	120	121	144	2.04E-87	248	99.17	82.64
	IBTHAUMO2_v1_1100079	IBTHAUMv1_4230002	100	172	172	354	6.57E-127	358	100.00	48.31
	IBTHAUMO2_v1_1110001	IBTHAUMv1_14670003	100	147	147	339	1.13E-106	305	100.00	43.07
	IBTHAUMO2_v1_20011	IBTHAUMv1_18170003	100	119	119	454	1.75E-82	246	100.00	25.99
Integrases	IBTHAUMO2_v1_240171	IBTHAUMv1_2410001	99.74	385	557	387	0	801	69.12	99.22
	IBTHAUMO2_v1_450024	IBTHAUMv1_16200001	100	454	454	472	0	939	100.00	95.97
	IBTHAUMO2_v1_730023	IBTHAUMv1_1500005	98.063	413	448	424	0	840	92.19	96.93
	IBTHAUMO2_v1_880010	IBTHAUMv1_16080009	99.787	469	469	469	0	967	100.00	99.79
	IBTHAUMO2_v1_780006	IBTHAUMv1_11050003	99.674	307	307	343	0	628	100.00	89.21
Restriction-modification systems	IBTHAUMO2_v1_1050026	IBTHAUMv1_1120001	25.738	237	927	640	2.47E-06	48.5	25.57	31.41
	IBTHAUMO2_v1_1130086	IBTHAUMv1_13350012	25.895	475	612	1038	8.26E-32	129	77.61	45.47
	IBTHAUMO2_v1_260066	IBTHAUMv1_14890001	99.05	421	1333	586	0	863	31.58	71.67
	IBTHAUMO2_v1_700006	IBTHAUMv1_4230001	100	887	953	889	0	1845	93.07	99.66
	IBTHAUMO2_v1_880011	IBTHAUMv1_13350012	20.659	334	908	1038	2.49E-06	48.9	36.78	31.21
	IBTHAUMO2_v1_890002	IBTHAUMv1_13350012	99.711	1038	1037	1038	0	2118	100.10	99.90
	IBTHAUMO2_v1_240074	IBTHAUMv1_15140004	99.184	490	490	490	0	975	100.00	99.80
	IBTHAUMO2_v1_240151	IBTHAUMv1_16180005	100	574	574	582	0	1178	100.00	98.45
	IBTHAUMO2_v1_280001	IBTHAUMv1_11110026	98.119	638	675	729	0	1280	94.52	87.38
	IBTHAUMO2_v1_380002	IBTHAUMv1_11240027	99.42	862	862	862	0	1708	100.00	99.88
	IBTHAUMO2_v1_730017	IBTHAUMv1_3930004	99.719	711	711	711	0	1407	100.00	99.86
	IBTHAUMO2_v1_800038	IBTHAUMv1_3940004	100	648	648	648	0	1320	100.00	99.85
	IBTHAUMO2_v1_260067	IBTHAUMv1_980001	97.107	242	271	273	1.02E-174	480	89.30	88.28
	IBTHAUMO2_v1_590086	IBTHAUMv1_1620001	35	60	854	856	3.10E-01	32	7.03	6.89
	IBTHAUMO2_v1_790008	IBTHAUMv1_19180002	90.868	438	439	442	0	823	99.77	98.87

IBTHAUMO2_v1_390013	IBTHAUMv1_14530025	99.27	274	290	283	0	559	94.48	96.47	
IBTHAUMO2_v1_590085	IBTHAUMv1_9460007	29.957	464	633	608	3.18E-52	187	73.30	63.65	
IBTHAUMO2_v1_590087	IBTHAUMv1_9460007	35.641	390	594	608	7.75E-62	213	65.66	59.38	
IBTHAUMO2_v1_740003	IBTHAUMv1_70001	66	450	446	477	0	639	100.90	94.13	
IBTHAUMO2_v1_320013	IBTHAUMv1_3540002	100	281	281	281	0	561	100.00	99.64	
IBTHAUMO2_v1_390007	IBTHAUMv1_14530029	98.233	283	299	287	0	558	94.65	98.26	
IBTHAUMO2_v1_770023	IBTHAUMv1_19010011	100	269	269	269	0	558	100.00	99.63	
IBTHAUMO2_v1_240101	IBTHAUMv1_10080009	99.569	464	510	467	0	925	90.98	99.14	
IBTHAUMO2_v1_590091	IBTHAUMv1_7470001	93.216	398	462	399	0	763	86.15	99.50	
IBTHAUMO2_v1_690028	IBTHAUMv1_3820007	30.699	329	377	379	8.32E-33	124	87.27	79.68	
IBTHAUMO2_v1_810008	IBTHAUMv1_7470001	45.013	391	474	399	1.25E-98	300	82.49	94.99	
Toxin: antitoxin systems	IBTHAUMO2_v1_1130060	IBTHAUMv1_13940004	100	83	83	83	2.73E-58	170	100.00	98.80
	IBTHAUMO2_v1_990027	IBTHAUMv1_13940004	34.667	75	86	83	2.83E-11	52	87.21	87.95
	IBTHAUMO2_v1_570004	IBTHAUMv1_840006	98.214	112	112	112	5.96E-77	220	100.00	99.11
	IBTHAUMO2_v1_590016	IBTHAUMv1_23220003	98.942	378	378	378	0	740	100.00	99.74
	IBTHAUMO2_v1_330015	IBTHAUMv1_1010002	99.091	330	377	330	0	655	87.53	99.70
	IBTHAUMO2_v1_520002	IBTHAUMv1_4560007	100	376	377	376	0	768	99.73	99.73
	IBTHAUMO2_v1_210021	IBTHAUMv1_6980001	100	294	402	294	0	598	73.13	99.66
	IBTHAUMO2_v1_440006	IBTHAUMv1_15080002	99.785	465	465	465	0	900	100.00	99.78
	IBTHAUMO2_v1_870005	IBTHAUMv1_5820001	100	214	447	216	1.21E-150	424	47.87	98.61
	IBTHAUMO2_v1_940001	IBTHAUMv1_4550011	100	418	419	465	0	835	99.76	89.68

Table S3. Expressed proteins assigned to the *I. basta* thaumarchaeote MAG ordered by NSAF value. Proteins that are encoded exclusively by *Ca. N. bastadiensis* among the AOA are labeled in orange. Proteins encoded by all AOA are labeled in blue.

Accession	Gene	Description	AA length	NSA F	OG Family	Presence in 454 Thaumarchaeal bin				Distribution of OGs**	Notes
						Accession	maxRap *	minRap *	% BLASTp hit		
IBTHAUMO2_v1_1100065		4Fe-4S ferredoxin	100	9.23%	OG0000047	IBTHAUMv1_12290026	1	1	100	Core	
IBTHAUMO2_v1_240128	tuf	Elongation factor 1-alpha	432	5.90%	OG00000743	IBTHAUMv1_310002	1	1	100	Core	
IBTHAUMO2_v1_720032	nirK	putative nitrite reductase, copper-dependent	468	3.95%	OG00000247	IBTHAUMv1_10010001	0.46795	0.99095	96.35	not in <i>Ca. N. islandicus</i> and <i>Ca. C. symbiosum</i>	
IBTHAUMO2_v1_320009	amoB	putative archaeal ammonia monooxygenase subunit B	189	3.49%	OG00000306	IBTHAUMv1_240002	1	1	100	Core	
IBTHAUMO2_v1_950017		conserved protein of unknown function	355	3.34%	OG0000097	IBTHAUMv1_4200003	0.58028	0.78626	89.32		
IBTHAUMO2_v1_890024	ths	Thermosome subunit	546	3.22%	OG00000022	IBTHAUMv1_7040001	1	1	99.82	Core	
IBTHAUMO2_v1_240148		Zn-dependent oxidoreductase	356	3.09%	OG00000035	IBTHAUMv1_16180002	1	1	100	Core	
IBTHAUMO2_v1_1130066		conserved protein of unknown function	86	3.07%	OG00001007	IBTHAUMv1_620009	1	1	100		
IBTHAUMO2_v1_1100022	ths	Thermosome subunit	566	3.03%	OG00000022	IBTHAUMv1_4580008	1	1	99.82	Core	
IBTHAUMO2_v1_510038	rpp41	Exosome complex component Rrp41	243	2.53%	OG00000833	IBTHAUMv1_1960004	1	1	100	Core	
IBTHAUMO2_v1_250013	trxA	Thioredoxin 1	108	2.44%	OG00000373	IBTHAUMv1_11050023	1	1	100	Core	
IBTHAUMO2_v1_170030	atpA	V-type ATP synthase alpha chain	589	2.39%	OG00000512	IBTHAUMv1_3990024	1	1	100	Core	
IBTHAUMO2_v1_320010	amoC	Ammonia monooxygenase/methane monooxygenase, subunit C	187	2.35%	OG00000065	IBTHAUMv1_4820001	0.92118	1	100	Core	
IBTHAUMO2_v1_1070007		Band 7 protein	285	2.31%	OG00001373	IBTHAUMv1_16780016	0.8807	1	100		
IBTHAUMO2_v1_1110035	psmA	Proteasome subunit alpha 2	240	1.83%	OG00000072	IBTHAUMv1_1190006	1	1	100	Core	
IBTHAUMO2_v1_270002		protein of unknown function	986	1.74%	OG0001421	IBTHAUMv1_16090001	0.91481	1	100	All 3 sponge symbionts, 2 <i>Ca. Nitrosotaleales</i> , 1 <i>Ca. N. brevis</i>	s-layer protein family
IBTHAUMO2_v1_780001		exported protein of unknown function	511	1.63%	OG0001421	IBTHAUMv1_2030001	0.48711	0.99804	100	All 3 sponge symbionts, 2 <i>Ca. Nitrosotaleales</i> , 1 <i>Ca. N. brevis</i>	s-layer protein family
IBTHAUMO2_v1_450045	sufC	FeS assembly ATPase SufC	256	1.55%	OG00000878	IBTHAUMv1_9550001	1	1	100	Core	
IBTHAUMO2_v1_1070037		4Fe-4S ferredoxin	181	1.46%	OG00000029	IBTHAUMv1_3930011	1	1	100	Core	
IBTHAUMO2_v1_1130095	livK	ABC-type branched-chain amino acid transport system, periplasmic component (modular protein)	526	1.42%	OG0001679	IBTHAUMv1_16960002	1	1.03137	93.73	All 3 sponge symbionts, <i>N. maritimus</i> and both <i>Nitrosocosmamus</i> spp.	
IBTHAUMO2_v1_660006		exported protein of unknown function	510	1.38%	OG0001421	IBTHAUMv1_2030001	0.48902	1.00392	82.62	All 3 sponge symbionts, 2 <i>Ca. Nitrosotaleales</i> , 1 <i>Ca. N. brevis</i>	s-layer protein family
IBTHAUMO2_v1_1030029		putative archaeal aspartate aminotransferase	383	1.38%	OG00000543	IBTHAUMv1_3950021	1	1	100	Core	
IBTHAUMO2_v1_240080		exported protein of unknown function	2072	1.32%	OG0001466	IBTHAUMv1_11360001	1	1	98.65	<i>Ca. N. bastadiensis</i> unique	DUF5011 domain-containing
IBTHAUMO2_v1_990028	psmA	Proteasome subunit alpha	244	1.26%	OG00000072	IBTHAUMv1_15240015	1	1	100	Core	
IBTHAUMO2_v1_60001		exported protein of unknown function	1110	1.23%	OG0001421	IBTHAUMv1_15240010	0.71754	1.05045	62.78	All 3 sponge symbionts, 2 <i>Ca. Nitrosotaleales</i> , 1 <i>Ca. N. brevis</i>	s-layer protein family

IBTHAUMO2_v1_320005	<i>rps15</i>	30S ribosomal protein S15	149	1.18%	OG0000795	IBTHAUMv1_240006	1	1	99.33	Core	
IBTHAUMO2_v1_170031	<i>atpB</i>	V-type ATP synthase beta chain	456	1.16%	OG0000511	IBTHAUMv1_3990023	1	1	100	Core	
IBTHAUMO2_v1_980016	<i>rpoA</i>	DNA-directed RNA polymerase subunit A''	1263	1.11%	OG0000600	IBTHAUMv1_12910016	1	1	100	Core	
IBTHAUMO2_v1_450036		protein of unknown function	82	1.07%	OG0002396	IBTHAUMv1_15190002	1	1	90.24	Only shared b/n <i>Ca. N. bastadiensis</i> , <i>N. maritimus</i> , and <i>Ca. N. gargensis</i>	
IBTHAUMO2_v1_950026	<i>ftnB</i>	putative ferritin-2	168	1.05%	OG0001406	IBTHAUMv1_3240002	1	1	99.4	Sporadic distribution - seems to be concentrated in the Nitrosopumiliaceae	
IBTHAUMO2_v1_530013	<i>albA</i>	DNA/RNA-binding protein Alba (modular protein)	170	1.03%	OG0000027	IBTHAUMv1_3270004	1	1	100	Core	
IBTHAUMO2_v1_980006	<i>mdh</i>	Malate dehydrogenase	302	1.02%	OG0000569	IBTHAUMv1_4300002	0.91515	1	98.34	Core	
IBTHAUMO2_v1_240105		conserved exported protein of unknown function	451	0.97%	OG0000059	IBTHAUMv1_1870005	0.55654	1	100		
IBTHAUMO2_v1_770040		Cyclase/dehydrase	198	0.89%	OG0000265	IBTHAUMv1_20630002	1	1	100	Core	
IBTHAUMO2_v1_980019		Ribosomal protein L7Ae/L30e/S12e/Gadd45	104	0.85%	OG0000601	IBTHAUMv1_12970010	1	1	100	Core	
IBTHAUMO2_v1_1110009		conserved exported protein of unknown function	313	0.84%	OG0000016	IBTHAUMv1_920001	0.85942	1	99.26	Core	
IBTHAUMO2_v1_1110029	<i>erpA</i>	Iron-sulfur cluster insertion protein ErpA 1	116	0.76%	OG0000603	IBTHAUMv1_18460002	1	1	100	Core	
IBTHAUMO2_v1_1110033	<i>gdhA</i>	Glutamate dehydrogenase	424	0.73%	OG0000604	IBTHAUMv1_18460006	0.80189	1	100	Core	
IBTHAUMO2_v1_990049	<i>rpl6</i>	50S ribosomal protein L6	182	0.72%	OG0000737	IBTHAUMv1_4350015	1	1	99.45	Core	
IBTHAUMO2_v1_720011		exported protein of unknown function	1424	0.71%	OG0001466	IBTHAUMv1_4130010	1	1	99.16	<i>Ca. N. bastadiensis</i> unique	
IBTHAUMO2_v1_470003	<i>tbp</i>	TATA-box-binding protein	187	0.71%	OG0000031	IBTHAUMv1_12200005	1	1	100	Core	
IBTHAUMO2_v1_240046		conserved protein of unknown function	130	0.68%	OG0000007	IBTHAUMv1_2100004	1	1	100	only missing in <i>Ca.N. islandicus</i>	
IBTHAUMO2_v1_980022	<i>rps7</i>	30S ribosomal protein S7	199	0.66%	OG0000837	IBTHAUMv1_13050003	1	1	100	Core	
IBTHAUMO2_v1_220008	<i>sodA</i>	Superoxide dismutase [Mn]	205	0.64%	OG0000084	IBTHAUMv1_13830025	1	1	100	Core	
IBTHAUMO2_v1_260024		Universal stress protein (UspA domain-containing protein)	141	0.62%	OG0000011	IBTHAUMv1_1640004	1	1	100	only missing in <i>Ca.N. islandicus</i>	important for oxidative and acid stress
IBTHAUMO2_v1_260038		Cupin 2 conserved barrel domain protein	142	0.62%	OG0001023	IBTHAUMv1_1140005	1	1	99.3	only missing in <i>Ca.N. islandicus</i>	
IBTHAUMO2_v1_340008	<i>dnaK</i>	Chaperone protein DnaK	503	0.61%	OG0000335	IBTHAUMv1_11380008	0.75262	0.99801	100	Core	
IBTHAUMO2_v1_210018	<i>cofD</i>	LPPG:FO 2-phospho-L-lactate transferase	306	0.57%	OG0000676	IBTHAUMv1_4620004	1	1	100	Core	F420 biosynthesis
IBTHAUMO2_v1_1110028	<i>dnaG</i>	DNA primase DnaG	386	0.57%	OG0000693	IBTHAUMv1_2640008	0.80829	1	99.68	Core	
IBTHAUMO2_v1_1030019	<i>ppi</i>	putative peptidyl-prolyl cis-trans isomerase	158	0.56%	OG0000324	IBTHAUMv1_12830004	1	1	100	only missing in <i>Ca.N. islandicus</i>	
IBTHAUMO2_v1_210017		conserved exported protein of unknown function	448	0.49%	OG0000096	IBTHAUMv1_1340002	1	1	100	Core	
IBTHAUMO2_v1_320015		Alkyl hydroperoxide reductase	182	0.48%	OG0000941	IBTHAUMv1_2320004	1	1	99.45	only missing in <i>Ca.N. salalaria</i>	
IBTHAUMO2_v1_240129	<i>fbp</i>	bifunctional fructose-1,6-bisphosphatase	376	0.47%	OG0000417	IBTHAUMv1_310001	0.97606	1	99.46	Core	
IBTHAUMO2_v1_1130058	<i>pepA</i>	putative leucyl aminopeptidase	477	0.46%	OG0001191	IBTHAUMv1_13940006	1	1	99.79	missing in <i>Ca. N. islandicus</i> and all <i>Ca. Nitrosotaleales</i>	
IBTHAUMO2_v1_720005	<i>rpoE</i>	DNA-directed RNA polymerase subunit E'	193	0.46%	OG0000408	IBTHAUMv1_4130016	1	1	100	Core	

IBTHAUMO2_v1_1130033	<i>accC/pccC</i>	acetyl-CoA/propionyl-CoA carboxylase, biotin carboxylase subunit	485	0.45%	OG0000362	IBTHAUMv1_13940030	1	1	100	Core	
IBTHAUMO2_v1_720031		NAD-binding D-isomer specific 2-hydroxyacid dehydrogenase	310	0.43%	OG0000385	IBTHAUMv1_4660002	1	1	97.42	Core	
IBTHAUMO2_v1_990024	<i>fusA</i>	Elongation factor 2	730	0.42%	OG0000645	IBTHAUMv1_16760020	1	1	99.73	Core	
IBTHAUMO2_v1_720043		exported protein of unknown function	1462	0.42%	OG0001466	IBTHAUMv1_5230001	0.70588	0.99807	95.35	<i>Ca. N. bastadiensis</i> unique	
IBTHAUMO2_v1_1100034		Peptidyl-prolyl cis-trans isomerase	533	0.41%	OG0000003	IBTHAUMv1_17580009	1	1	99.25	only missing in both <i>Nitrosocosmus</i> spp.	
IBTHAUMO2_v1_40002		conserved protein of unknown function	976	0.41%	OG0000006	IBTHAUMv1_3870008	0.61226	1.03381	75.22	only missing in both <i>Nitrosocosmus</i> spp.	s-layer protein family
IBTHAUMO2_v1_240132		conserved protein of unknown function	217	0.41%	OG0000436	IBTHAUMv1_5220002	1	1	100	Core	contains PF01865 domain - putative phosphate transport regulator
IBTHAUMO2_v1_1080008		exported protein of unknown function	557	0.39%	OG0001421	IBTHAUMv1_15240001	0.33504	0.93896	62.33	All 3 sponge symbionts, 2 <i>Ca. Nitrosotaleales</i> , 1 <i>Ca. N. brevis</i>	s-layer protein family
IBTHAUMO2_v1_240136		Short-chain dehydrogenase/reductase SDR	574	0.38%	OG0000810	IBTHAUMv1_1110007	1	1	99.48	Core	
IBTHAUMO2_v1_980023		membrane protein of unknown function	586	0.38%	OG0011727	IBTHAUMv1_12910009	1	1	99.83	singleton	
IBTHAUMO2_v1_1110030		3-hydroxypropionyl-CoA dehydratase/Crotonyl-CoA hydratase [(S)-3-hydroxybutyryl-CoA forming]	252	0.35%	OG0000227	IBTHAUMv1_18460003	1	1	100	Core	
IBTHAUMO2_v1_510039	<i>rrp42</i>	Exosome complex component Rrp42	270	0.33%	OG0000834	IBTHAUMv1_1960005	1	1	100	Core	
IBTHAUMO2_v1_110023	<i>glyA</i>	Serine hydroxymethyltransferase	448	0.29%	OG0000541	IBTHAUMv1_4580009	0.97545	1	100	Core	
IBTHAUMO2_v1_940015	<i>sucD</i>	succinyl-CoA synthetase, NAD(P)-binding, alpha subunit	302	0.29%	OG0000763	IBTHAUMv1_330006	1	1	99.34	Core	
IBTHAUMO2_v1_590109	<i>sufD</i>	FeS assembly protein	461	0.29%	OG0000995	IBTHAUMv1_4640007	1	1	100	only missing in <i>Ca.N. salalaria</i>	
IBTHAUMO2_v1_800011		putative aldolase	314	0.28%	OG0000682	IBTHAUMv1_1460002	1	1.0129	98.73	Core	putatively functional in E.C. 4.1.2.13
IBTHAUMO2_v1_590122	<i>hemB</i>	Delta-aminolevulinic acid dehydratase	321	0.27%	OG0000183	IBTHAUMv1_830005	0.85981	1	100	Core	
IBTHAUMO2_v1_260012	<i>trxB</i>	Thioredoxin reductase	327	0.27%	OG0000820	IBTHAUMv1_4840006	0.93162	1	99.69	Core	
IBTHAUMO2_v1_1080004		conserved exported protein of unknown function	508	0.26%	OG0000016	IBTHAUMv1_16190003	1	1	99.41	Core	
IBTHAUMO2_v1_170024		H(+) -transporting two-sector ATPase	340	0.26%	OG0000137	IBTHAUMv1_2710003	1	1	100	Core	
IBTHAUMO2_v1_950011	<i>aroB</i>	3-dehydroquinate synthase	341	0.26%	OG0000823	IBTHAUMv1_560007	1	1	96.19	Core	tyrosine, tryptophan, phe synthesis
IBTHAUMO2_v1_170028	<i>atpl</i>	V-type ATP synthase subunit I	694	0.25%	OG0001210	IBTHAUMv1_15570002	0.62104	1	100	Core	
IBTHAUMO2_v1_1110031		3-Hydroxypropionyl-CoA synthetase	704	0.25%	OG0000680	IBTHAUMv1_18460004	1	1	100	Core	
IBTHAUMO2_v1_770013		AAA family ATPase, CDC48 subfamily	728	0.24%	OG0000098	IBTHAUMv1_11430014	1	1	100	Core	
IBTHAUMO2_v1_300003		Redoxin domain-containing protein	371	0.24%	OG0000167	IBTHAUMv1_13230016	1	1	99.73	only missing in <i>Ca.N. islandicus</i>	
IBTHAUMO2_v1_470029		Beta-lactamase domain-containing protein	421	0.21%	OG0000769	IBTHAUMv1_1130003	1	1	99.76	Core	
IBTHAUMO2_v1_260042	<i>hemL</i>	Glutamate-1-semialdehyde 2,1-aminomutase 2	441	0.20%	OG0000389	IBTHAUMv1_13740001	0.92517	0.99756	99.75	Core	F430/tetrapyrrole/B12 biosynthesis
IBTHAUMO2_v1_980015	<i>rpoB</i>	DNA-directed RNA polymerase subunit B	1115	0.20%	OG0000599	IBTHAUMv1_1480002	0.71031	0.99874	99.87	Core	
IBTHAUMO2_v1_370006	<i>cysM</i>	Cysteine synthase	492	0.18%	OG0001268	IBTHAUMv1_12200010	1	1	98.78	missing in <i>Ca. N. islandicus</i> , both <i>Nitrosocosmus</i> spp., all <i>Ca. Nitrosotenuaceae</i>	

IBTHAUMO2_v1_690011		conserved exported protein of unknown function	492	0.18%	OG0000003	IBTHAUMv1_11050007	1	1	99.59	not in both Nitrosocosmics and many AOA have multiple copies	SSF51004: Cytochrome cd1-nitrite reductase-like, haem d1 domain superfamily
IBTHAUMO2_v1_320044	<i>aco</i>	Aconitate hydratase	745	0.18%	OG0000268	IBTHAUMv1_4090010	1	1	99.46	Core	
IBTHAUMO2_v1_370005		von Willebrand factor type A	498	0.18%	OG0000623	IBTHAUMv1_12200011	0.58635	1	99.66	Core	COG4548: P, Nitric oxide reductase activation protein
IBTHAUMO2_v1_330024	<i>pstS</i>	ABC-type phosphate transport system periplasmic component (PstS)	508	0.17%	OG0000113	IBTHAUMv1_17840008	1	1	99.41	missing in <i>Ca. N. salaria</i> , <i>Ca.N. koreensis</i> AR2, <i>Ca. N. sediminis</i> , and <i>Ca. N. catalina</i>	
IBTHAUMO2_v1_170026	<i>amt2</i>	Ammonium transporter	520	0.17%	OG0000221	IBTHAUMv1_15380013	0.96923	1	100	missing in both Nitrosocosmics spp.	
IBTHAUMO2_v1_620022		protein of unknown function	1844	0.17%	OG0001466	IBTHAUMv1_12370012	0.85016	1	98.86	<i>Ca. N. bastadiensis</i> unique	DUF5011 domain-containing
IBTHAUMO2_v1_960004	<i>ths</i>	Thermosome subunit	560	0.16%	OG0002000	IBTHAUMv1_4580008	0.89223	0.90179	42.57		
IBTHAUMO2_v1_530015	<i>sdhA</i>	Succinate dehydrogenase or fumarate reductase, flavoprotein subunit	570	0.15%	OG0000437	IBTHAUMv1_4000002	0.92632	1	98.48	Core	
IBTHAUMO2_v1_590087		Type III restriction-modification system methyltransferase	593	0.15%	OG0001596	IBTHAUMv1_9460007	0.95058	0.97302	31.37		
IBTHAUMO2_v1_240089	<i>ppdK</i>	Pyruvate, phosphate dikinase	884	0.10%	OG0001061	IBTHAUMv1_4310008	1	1	100		
IBTHAUMO2_v1_700001		protein of unknown function	3094	0.10%	OG0001466	IBTHAUMv1_20360004	0.50517	0.96125	99.42	<i>Ca. N. bastadiensis</i> unique	DUF5011 domain-containing
IBTHAUMO2_v1_880008		exported protein of unknown function	2027	0.04%	OG0000017	IBTHAUMv1_19190004	0.32215	0.88243	46.86		putative M72 metalloendopeptidase

*These values are ratios of alignment lengths computed for each comparison using the BLAST software :

minLrap = Lmatch/min(Lprot1, Lprot2)

maxLrap = Lmatch/max(Lprot1, Lprot2)

where Lmatch = length of the match, Lprot1 = length of protein 1, Lprot2 = length of protein 2

if minLrap=1 and maxLrap=1 => the 2 proteins both align on their whole length

if minLrap=1 and maxLrap<1 => one of the proteins is longer than the other, or the alignment is partial.

singletons refer to genes which did not have a hit above an expected threshold in OrthoFinder amongst all queried sequences

**If certain AOA do not have members in certain orthologous groups it does not mean that a more distant homologous gene is not present

Table S4. Comparison of net nitrite formation and nitrification rates from our study with previously published sponge studies.

Sponge species	Net nitrification rates [μmol N (cm ⁻³ or g ⁻¹ wet wt.) day ⁻¹]	Net nitrite formation rates [μmol N (cm ⁻³ or g ⁻¹ wet wt.) day ⁻¹]	Marine area, depth, and season	Experimental Setup	AOB/AOA Diversity	Reference
<i>Anthosigmella varians</i>	0.003 – 0.105 (g ⁻¹ *)	N.D.	Caribbean coral reef (6m)	4h - 2.25 L batch incubations +/- light and 5 μM NH ₄ ⁺	N.D.	Corredor <i>et al.</i> , 1988
<i>Chondrilla nucula</i>	1.03 – 1.49 ◊ (g ⁻¹ *)					
<i>Chondrilla nucula</i>	0.864 – 6.36 (g ⁻¹ *)	0.014 – 0.24 (g ⁻¹ *)	Caribbean coral reef	6 to 12h – 3 and 20L batch inc., +/- light	N.D.	Diaz & Ward, 1997
<i>Pseudaxinella zeari</i>	0 – 2.47 (g ⁻¹ *)	0 – 0.048 (g ⁻¹ *)	(20-40m) and mangroves (1-3m);			
<i>Oligoceras violacea</i>	0 – 1.37 (g ⁻¹ *)	0.408 – 1.39 (g ⁻¹ *)				
<i>Plakortis halichondroides</i>	0 – 0.768 (g ⁻¹ *)	0 – 0.192 (g ⁻¹ *)	June-Sept.			
<i>Alphysina aerophoba</i>	3.6 – 9.2 ◊ (g ⁻¹)	N.D.	Med. Sea, 2-20m;	9 to 28h - 3L batch, +/- 100 or 200 μM NH ₄ ⁺	β-AOB 16S – 9 OTUs – 1 OTU	Bayer <i>et al.</i> , 2007
<i>Dysidea avara</i>	0					
<i>Chondrosia reniformis</i>	~0.3 (g ⁻¹)					
<i>Alphysina aerophoba</i>	0.214 – 0.826 (g ⁻¹ *)	N.D.	Med. Sea, 2-15m April - Sept.	21 to 28h – 3L batch inc., +/- 100 or 200 μM NH ₄ ⁺ +/- nitrapyrin	A- and β- <i>amoA</i> /16S – 5, 7, 9 OTUs	Bayer <i>et al.</i> , 2008
<i>Aplysina aerophoba</i>	1.13 (g ⁻¹ *)	N.D.	Med. Sea, 10-20m;	6h – 7L batch inc.		
<i>Agelas oroides</i>	0.875 (g ⁻¹ *)		Sept. for all except for <i>A. oroides</i> (July)		6 A- <i>amoA</i> OTUs in 3 clust.	Jiménez & Ribes, 2007; Ribes <i>et al.</i> , 2012
<i>Dysidea avara</i>	N.S.				12 β- <i>amoA</i> OTUs in 3 clust.	
<i>Chondroisa reniformis</i>	1.68 (g ⁻¹ *)				83 γ- <i>amoA</i> clones	
<i>Axinella polypoides</i>	0.452 (g ⁻¹ *)					
<i>Ircinia oros</i>	0.544 (g ⁻¹ *)					
<i>Aplysina cauliformis</i>	4.08 (g ⁻¹ *)	N.D.	Florida Keys, ~4m	6 to 8h – 2-4L batches; <i>in situ</i> sampling	N.D.	Southwell <i>et al.</i> , 2008
<i>Smenospongia aurea</i>	4.32 (g ⁻¹ *)					
7 other species: <i>A. archeri</i> , <i>A. lacunose</i> , <i>I. felix</i> , <i>I. strobilina</i> , <i>P. crassa</i> , <i>V. rigidia</i> , and <i>X. muta</i>	+++ + + + +					
<i>Chondrosia reniformis</i> , <i>Dysidea avara</i>	0.176 (g ⁻¹) 0.294 (g ⁻¹)	0.016 (g ⁻¹) 0.016 (g ⁻¹)	Med. Sea, 10-15m	24h – 1L batches with 10 μM NH ₄ ⁺	1 A- <i>amoA</i> OTU	Schlüppy <i>et al.</i> , 2010
<i>Phakellia ventilarium</i>	0.14 – 2.26 (g ⁻¹ ○)	0 – 0.192 (g ⁻¹ ○)	Norwegian coast	24 to 48 h in 500 to 900 mL	3 A- <i>amoA</i> OTUs	
<i>Antho dichotoma</i>	0.	0.360 (g ⁻¹ ○)	(fjords), 200-300m;	batches with 10-12 μM NH ₄ ⁺	3 A- <i>amoA</i> OTUs	Radax <i>et al.</i> , 2012; Hoffmann <i>et al.</i> , 2009
<i>Geodia barretti</i>	0.679 (g ⁻¹ ○)	0.180 (g ⁻¹ ○)	Mar.-Nov.		1 A- <i>amoA</i> OTU	
<i>Ianthella basta</i>	1.67 – 11.3 (g ⁻¹) 1.54 – 13.3 ◊ (g ⁻¹)	0.64 – 6.07 (g ⁻¹) 0.35 – 10.36 ◊ (g ⁻¹)	Coral Sea, Australia, 10 m; Sept. – Oct.	7- day long 24 h batch incubations in 1.74 L +/- 25, 100 μM NH ₄ ⁺ +/- PTIO	1 A- <i>amoA</i> OTU	This study

(*) signifies that sponge dry wt. g⁻¹ was converted by assuming dry weight = 10% of wet weight while a (○) signifies that sponge cm⁻³ was converted by assuming 1 cm³ sponge = 1.2 g wet weight sponge (Schlüppy *et al.*, 2010). A (◊) denotes that the rate is a potential rate (i.e. with added ammonium). A (+) indicates positive NO_x⁻ production where quantity was not assessed. “A-, β-, and γ-*amoA*” refer to archaeal, betaproteobacterial and gammaproteobacterial *amoA* OTUs, respectively.

Table S5. AOA used for comparative genome analyses.

Organism/Name	Assembly Accession	doi	Size (Mb)	GC%	Status	BioProject Accession	BioSample Accession	Strain	Completeness	Contamination
<i>Candidatus Nitrosocaldus icelandicus</i>	GCF_002906225.1	doi: https://doi.org/10.1101/235028	1.62	41.5	Complete Genon	PRJNA413650	SAMN07759886	3F	100	0
<i>Nitrosopumilus maritimus</i> SCM1	GCA_000018465.1	doi: 10.1073/pnas.0913533107	1.65	34.2	Complete Genon	PRJNA19265	SAMN00000032	SCM1	100	0.97
<i>Candidatus Cenarchaeum symbiosum</i> A	GCA_000200715.1	doi: 10.1073/pnas.0608549103	2.05	57.4	Chromosome	PRJNA202	SAMN02744041	-	99.03	0
<i>Candidatus Nitrosoarchaeum limnia</i> SFB1	GCA_000204585.1	doi: 10.1371/journal.pone.0016626	1.77	32.6	Chromosome	PRJNA52465	SAMN0247010	SFB1	98.06	0
<i>Candidatus Nitrosoarchaeum koreensis</i> MY1	GCA_000220175.2	doi: 10.1128/B.05717-11	1.61	32.7	Contig	PRJNA67913	SAMN02470178	MY1	100	0
<i>Candidatus Nitrosopumilus</i> salaria BD31	GCA_000242875.3	doi: 10.1128/B.00013-12	1.57	33.8	Contig	PRJNA50075	SAMN0016669	BD31	92.39	1.94
<i>Candidatus Nitrosopumilus</i> koreensis AR1	GCA_000293965.1	doi: 10.1128/B.01857-12	1.64	34.2	Complete Genon	PRJNA174387	SAMN02603137	AR1	94.66	0
<i>Candidatus Nitrosopumilus</i> sediminis	GCA_000299395.1	doi: 10.1128/B.01869-12	1.69	33.6	Complete Genon	PRJNA174388	SAMN02603138	AR2	97.09	0
<i>Candidatus Nitrosphaera</i> gargensis Ga9.2	GCA_000303155.1	doi: 10.1111/j.1462-2920.2012.02893.x	2.83	48.3	Complete Genon	PRJNA60505	SAMN02603264	-	100	2.91
<i>Candidatus Nitrosotenuis</i> chungbukensis	GCA_000685395.1	doi: 10.1128/AEM.03730-13	1.76	41.8	Contig	PRJNA210247	SAMN02767256	MY2	99.03	0.97
<i>Nitrosphaera viennensis</i> EN76	GCA_000698785.1	doi: 10.1093/ijs/0.063172-0	2.53	52.7	Complete Genon	PRJEA60103	SAMN02721150	EN76	100	0.97
<i>Candidatus Nitrosotenuis</i> uzonensis N4	GCA_000723185.1	doi: 10.1371/journal.pone.0080835	1.64	42.2	Contig	PRJEB4650	SAMEA3139018	N4	100	0.97
<i>Candidatus Nitrosphaera</i> evergladensis SR1	GCA_000730285.1	doi: 10.1371/journal.pone.0101648	2.95	50.1	Complete Genon	PRJNA235208	SAMN03081530	-	100	2.91
<i>Candidatus Nitrosocosmicus</i> oleophilus	GCA_000802205.2	doi: 10.1111/1758-2229.12477	3.43	34.1	Complete Genon	PRJNA210256	SAMN03074222	MY3	98.06	0.97
<i>Candidatus Nitrosopelagicus</i> brevis	GCA_000812185.1	doi: 10.1073/pnas.1416223112	1.23	33.2	Complete Genon	PRJNA223412	SAMN03273964	CN25	99.51	0
<i>Candidatus Nitrosopumilus</i> piranensis	GCA_000875775.1	doi: 10.1038/ismej.2015.200	1.71	33.8	Complete Genon	PRJNA269924	SAMN03257648	D3C	100	0.97
<i>Candidatus Nitrosotenuis</i> cloacae	GCA_000955905.3	doi: 10.1038/srep23747	1.62	41.0	Complete Genon	PRJNA272771	SAMN03286947	SAT1	100	1.94
<i>Candidatus Nitrosopumilus</i> adriaticus	GCA_000956175.1	doi: 10.1038/ismej.2015.200	1.80	33.4	Complete Genon	PRJNA269341	SAMN03253153	NF5	100	0
<i>Candidatus Nitrosopumilus</i> sp. Nsub (glass sponge MAG)	GCA_001541925.1	doi: 10.1128/mSystems.00184-16	1.38	31.4	Contig	PRJNA308059	SAMN04386402	Nsub	100	0
<i>Candidatus Nitrosocosmicus</i> exaquare	GCA_001870125.1	doi: 10.1038/ismej.2016.192	2.99	33.9	Complete Genon	PRJNA317395	SAMN04606696	G61	99.03	2.91
<i>Candidatus Nitrosomarinus</i> catalina	GCA_002156965.1	doi: 10.1111/1462-2920.13768	1.36	31.4	Complete Genon	PRJNA341864	SAMN05730076	SPOT01	100	0
<i>Candidatus Nitrosotenuis</i> aquarius AQ6F	GCA_002787055.1	doi: 10.1128/AEM.01430-18	1.70	42.2	Complete Genon	PRJNA406986	SAMN07637255	AQ6F	99.68	1.94
<i>Candidatus Nitrosotalea</i> devanaterra	GCA_900065925.1	doi: 10.1128/AEM.04031-15	1.81	37.1	Complete Genon	PRJEB10948	SAMEA3577360	-	98.54	0
<i>Candidatus Nitrosotalea</i> sinensis Nd2	GCA_900143675.1	doi: 10.1111/1462-2920.13971	1.60	37.4	Contig	PRJEB15449	SAMEA20449918	-	99.51	0.97
<i>Candidatus Nitrosotalea</i> bavarica SbT1	GCA_900167955.1	doi: 10.1111/1462-2920.13971	1.55	36.0	Scaffold	PRJEB15449	SAMEA101071168	-	97.57	1.94
<i>Candidatus Nitrosotalea</i> okcheonensis CS	GCA_900177045.1	doi: 10.1111/1462-2920.13971	1.97	37.5	Chromosome	PRJEB15449	SAMEA20449168	-	99.51	0
CcThau Ga0078905 (Sponge MAG)	IMG_2626541593_protein	doi: 10.1038/ismej.2017.25	2.16	38.4	Contig	NA	NA	-	97.12	4.01
<i>Candidatus Nitrosospongia</i> bastadiensis	NA	This publication	1.99	64.8	Scaffold	PRJEB29556	SAMEA5126984	O2	99.03	0.97

References

- Bayer, K., Schmitt, S., and Hentschel, U. (2007) Microbial nitrification in Mediterranean sponges: possible involvement of ammonium-oxidizing *Betaproteobacteria*. In *Porifera Research: Biodiversity, Innovation, Sustainability*. Custódio, M., Lôbo-Hajdu, G., Hajdu, E., and Muricy, G. (eds). Série Livros. Rio de Janeiro, Brazil: Museu Nacional, pp. 165–171.
- Bayer, K., Schmitt, S., and Hentschel, U. (2008) Physiology, phylogeny and *in situ* evidence for bacterial and archaeal nitrifiers in the marine sponge *Aplysina aerophoba*. *Environ Microbiol* **10**: 2942–2955.
- Berger, S.A., Krompass, D., and Stamatakis, A. (2011) Performance, accuracy, and web Server for evolutionary placement of short sequence reads under maximum-likelihood. *Syst Biol* **60**: 291–302.
- Blatch, G.L. and Lässle, M. (1999) The tetratricopeptide repeat: a structural motif mediating protein-protein interactions. *Bioessays* **21**: 932–939.
- Callebaut, I., Mornon, J.-P., Gilgès, D., and Vigon, I. (2000) HYR, an extracellular module involved in cellular adhesion and related to the immunoglobulin-like fold. *Protein Sci* **9**: 1382–1390.
- Camacho, C., Coulouris, G., Avagyan, V., Ma, N., Papadopoulos, J., Bealer, K., and Madden, T.L. (2009) BLAST+: architecture and applications. *BMC Bioinformatics* **10**: 421.
- Capella-Gutierrez, S., Silla-Martinez, J.M., and Gabaldon, T. (2009) trimAl: a tool for automated alignment trimming in large-scale phylogenetic analyses. *Bioinformatics* **25**: 1972–1973.
- Cort, J.R., Yee, A., Edwards, A.M., Arrowsmith, C.H., and Kennedy, M.A. (2000) Structure-based functional classification of hypothetical protein MTH538 from *Methanobacterium thermoautotrophicum*. *J Mol Biol* **302**: 189–203.
- Corredor, J.E., Wilkinson, C.R., Vicente, V.P., Morell, J.M., and Otero, E. (1988) Nitrate release by Caribbean reef sponges. *Limnol Oceanogr* **33**: 114–120.
- Diaz, M. and Ward, B. (1997) Sponge-mediated nitrification in tropical benthic communities. *Mar Ecol Prog Ser* **156**: 97–107.
- Doron, S., Melamed, S., Ofir, G., Leavitt, A., Lopatina, A., Keren, M., et al. (2018) Systematic discovery of antiphage defense systems in the microbial pangenome. *Science* **359**: eaar4120.

- Fan, L., Reynolds, D., Liu, M., Stark, M., Kjelleberg, S., Webster, N.S., and Thomas, T. (2012)
185 Functional equivalence and evolutionary convergence in complex communities of
microbial sponge symbionts. *Proc Natl Acad Sci USA* **109**: E1878–E1887.
- Foerstner, K.U., von Mering, C., Hooper, S.D., and Bork, P. (2005) Environments shape the
nucleotide composition of genomes. *EMBO Rep* **6**: 1208–1213.
- Gauthier, M.E.A., Du Pasquier, L., and Degnan, B.M. (2010) The genome of the sponge
190 Amphimedon queenslandica provides new perspectives into the origin of Toll-like and
interleukin 1 receptor pathways: The origin of Toll-like and IL1 receptor pathways. *Evol
Dev* **12**: 519–533.
- Herbold, C.W., Lehtovirta-Morley, L.E., Jung, M.-Y., Jehmlich, N., Hausmann, B., Han, P., *et al.* (2017) Ammonia-oxidising archaea living at low pH: Insights from comparative
195 genomics: Comparative genomics of ammonia-oxidising archaea. *Environ Microbiol* **19**:
4939–4952.
- Hoffmann, F., Radax, R., Woebken, D., Holtappels, M., Lavik, G., Rapp, H.T., *et al.* (2009)
Complex nitrogen cycling in the sponge *Geodia barretti*. *Environ Microbiol* **11**: 2228–
2243.
- 200 Horn, H., Slaby, B.M., Jahn, M.T., Bayer, K., Moitinho-Silva, L., Förster, F., *et al.* (2016) An
enrichment of CRISPR and other defense-related features in marine sponge-associated
microbial metagenomes. *Front Microbiol* **7**: 1751.
- Huerta-Cepas, J., Szklarczyk, D., Forslund, K., Cook, H., Heller, D., Walter, M.C., *et al.*
(2016) eggNOG 4.5: a hierarchical orthology framework with improved functional
205 annotations for eukaryotic, prokaryotic and viral sequences. *Nucleic Acids Res* **44**: D286–
D293.
- Jiménez, E. and Ribes, M. (2007) Sponges as a source of dissolved inorganic nitrogen:
Nitrification mediated by temperate sponges. *Limnol Oceanogr* **52**: 948–958.
- Kalyaanamoorthy, S., Minh, B.Q., Wong, T.K.F., von Haeseler, A., and Jermiin, L.S. (2017)
210 ModelFinder: fast model selection for accurate phylogenetic estimates. *Nat Methods* **14**:
587–589.
- Katoh, K. and Standley, D.M. (2013) MAFFT Multiple Sequence Alignment Software Version
7: Improvements in Performance and Usability. *Mol Biol Evol* **30**: 772–780.
- Kerou, M., Offre, P., Valledor, L., Abby, S.S., Melcher, M., Nagler, M., *et al.* (2016)
215 Proteomics and comparative genomics of *Nitrososphaera viennensis* reveal the core
genome and adaptations of archaeal ammonia oxidizers. *Proc Natl Acad Sci USA* **113**:
E7937–E7946.

- 220 Lagkouvardos, I., Joseph, D., Kapfhammer, M., Giritli, S., Horn, M., Haller, D., and Clavel, T. (2016) IMNGS: A comprehensive open resource of processed 16S rRNA microbial profiles for ecology and diversity studies. *Sci Rep-UK* **6**: 33721.
- 225 Lassalle, F., Périan, S., Bataillon, T., Nesme, X., Duret, L., and Daubin, V. (2015) GC-Content evolution in bacterial genomes: the biased gene conversion hypothesis expands. *PLoS Genet* **11**: e1004941.
- Laundon, D., Larson, B., McDonald, K., King, N., and Burkhardt, P. (2018) The architecture of
225 cell differentiation in choanoflagellates and sponge choanocytes. *bioRxiv*.
- Li, P.-N., Herrmann, J., Tolar, B.B., Poitevin, F., Ramdasi, R., Bargar, J.R., et al. (2018) Nutrient transport suggests an evolutionary basis for charged archaeal surface layer proteins. *ISME J* **12**: 2389–2402.
- Mah, J.L., Christensen-Dalsgaard, K.K., and Leys, S.P. (2014) Choanoflagellate and
230 choanocyte collar-flagellar systems and the assumption of homology. *Evol Dev* **16**: 25–37.
- Maldonado, M. (2005) Choanoflagellates, choanocytes, and animal multicellularity. *Invertebr Biol* **123**: 1–22.
- Manning, G., Young, S.L., Miller, W.T., and Zhai, Y. (2008) The protist, *Monosiga brevicollis*, has a tyrosine kinase signaling network more elaborate and diverse than found in any known metazoan. *Proc Natl Acad Sci USA* **105**: 9674–9679.
- 235 Moitinho-Silva, L., Díez-Vives, C., Batani, G., Esteves, A.I., Jahn, M.T., and Thomas, T. (2017) Integrated metabolism in sponge–microbe symbiosis revealed by genome-centered metatranscriptomics. *ISME J* **11**: 1651–1666.
- Moitinho-Silva, L., Nielsen, S., Amir, A., Gonzalez, A., Ackermann, G.L., Cerrano, C., et al.
240 (2017) The sponge microbiome project. *GigaScience* **6**: 1–7.
- Nguyen, L.-T., Schmidt, H.A., von Haeseler, A., and Minh, B.Q. (2015) IQ-TREE: a fast and effective stochastic algorithm for estimating maximum-likelihood phylogenies. *Mol Biol Evol* **32**: 268–274.
- Palatinszky, M., Herbold, C., Jehmlich, N., Pogoda, M., Han, P., von Bergen, M., et al. (2015)
245 Cyanate as an energy source for nitrifiers. *Nature* **524**: 105–108.
- Patterson, N.J., Günther, J., Gibson, A.J., Offord, V., Coffey, T.J., Splitter, G., et al. (2014) Two TIR-like domain containing proteins in a newly emerging zoonotic *Staphylococcus aureus* strain sequence type 398 are potential virulence factors by impacting on the host innate immune response. *Front Microbiol* **5**: 662.
- 250 Pruesse, E., Peplies, J., and Glöckner, F.O. (2012) SINA: Accurate high-throughput multiple sequence alignment of ribosomal RNA genes. *Bioinformatics* **28**: 1823–1829.

- Qin, W., Meinhardt, K.A., Moffett, J.W., Devol, A.H., Virginia Armbrust, E., Ingalls, A.E., and Stahl, D.A. (2017) Influence of oxygen availability on the activities of ammonia-oxidizing archaea. *Environ Microbiol Rep* **9**: 250–256.
- 255 Radax, R., Hoffmann, F., Rapp, H.T., Leininger, S., and Schleper, C. (2012) Ammonia-oxidizing archaea as main drivers of nitrification in cold-water sponges. *Environ Microbiol* **14**: 909–923.
- 260 Reichenberger, E.R., Rosen, G., Hershberg, U., and Hershberg, R. (2015) Prokaryotic nucleotide composition is shaped by both phylogeny and the environment. *Genome Biol Evol* **7**: 1380–1389.
- Reynolds, D. and Thomas, T. (2016) Evolution and function of eukaryotic-like proteins from sponge symbionts. *Mol Ecol* **25**: 5242–5253.
- 265 Ribes, M., Jiménez, E., Yahel, G., López-Sendino, P., Diez, B., Massana, R., et al. (2012) Functional convergence of microbes associated with temperate marine sponges. *Environ Microbiol* **14**: 1224–1239.
- Saier, M.H., Yen, M.R., Noto, K., Tamang, D.G., and Elkan, C. (2009) The Transporter Classification Database: recent advances. *Nucleic Acids Res* **37**: D274–D278.
- 270 Santoro, A.E., Dupont, C.L., Richter, R.A., Craig, M.T., Carini, P., McIlvin, M.R., et al. (2015) Genomic and proteomic characterization of “*Candidatus Nitrosopelagicus brevis*”: An ammonia-oxidizing archaeon from the open ocean. *Proc Natl Acad Sci USA* **112**: 1173–1178.
- Schläppy, M.-L., Schöttner, S.I., Lavik, G., Kuypers, M.M.M., de Beer, D., and Hoffmann, F. (2010) Evidence of nitrification and denitrification in high and low microbial abundance sponges. *Mar Biol* **157**: 593–602.
- 275 Shigeno-Nakazawa, Y., Kasai, T., Ki, S., Kostyanovskaya, E., Pawlak, J., Yamagishi, J., et al. (2016) A pre-metazoan origin of the CRK gene family and co-opted signaling network. *Sci Rep-UK* **6**: 3439.
- Southwell, M.W., Popp, B.N., and Martens, C.S. (2008) Nitrification controls on fluxes and isotopic composition of nitrate from Florida Keys sponges. *Mar Chem* **108**: 96–108.
- 280 Srivastava, M., Simakov, O., Chapman, J., Fahey, B., Gauthier, M.E.A., Mitros, T., et al. (2010) The *Amphimedon queenslandica* genome and the evolution of animal complexity. *Nature* **466**: 720–726.
- Stamatakis, A. (2014) RAxML version 8: a tool for phylogenetic analysis and post-analysis of large phylogenies. *Bioinformatics* **30**: 1312–1313.
- 285 Tian, R.-M., Sun, J., Cai, L., Zhang, W.-P., Zhou, G.-W., Qiu, J.-W., and Qian, P.-Y. (2016) The deep-sea glass sponge *Lophophysema eversa* harbours potential symbionts responsible

for the nutrient conversions of carbon, nitrogen and sulfur. *Environ Microbiol* **18**: 2481–2494.

290 Wang, H.-C., Susko, E., and Roger, A.J. (2006) On the correlation between genomic G+C content and optimal growth temperature in prokaryotes: Data quality and confounding factors. *Biochem Biophys Res Commun* **342**: 681–684.

Wiens, M., Korzhev, M., Perovic-Ottstadt, S., Luthringer, B., Brandt, D., Klein, S., and Muller, W.E.G. (2006) Toll-like receptors are part of the innate immune defense system of sponges (demospongiae: Porifera). *Mol Biol Evol* **24**: 792–804.

295 Wiens, M., Korzhev, M., Krasko, A., Thakur, N.L., Perović-Ottstadt, S., Breter, H.J., et al. (2005) Innate immune defense of the sponge *Suberites domuncula* against bacteria involves a MyD88-dependent signaling pathway: Induction of a perforin-like molecule. *J Biol Chem* **280**: 27949–27959.

300